UNITED STATES DEPARTMENT OF THE INTERIOR

GEOLOGICAL SURVEY

Discrimination of Alteration in the Crooks Gap, Wyoming Uranium District using Laboratory and Landsat Spectral Reflectance Data

by

Timothy E. Townsend

Open-File Report 79-765

1979

Table of Contents

Acknowledgments

The acknowledgments given here amply demonstrate that research is not carried out in a vacuum and that much is owed by the author to others whose help, comments, and criticism have improved this work manyfold.

In particular, many members of the U.S. Geological Survey in Denver, Colorado, deserve special thanks: Terry W. Offield, from whose initial investigations this thesis grew, and who provided help and advice throughout; Gary L. Raines, who provided guidance and criticism during the summer of 1977 and visited the author in the field; Phoebe L. Hauff, who trained the author in X-ray analysis of clay minerals and interpreted the resulting data with the help of Paul D. Blackmon and Harry C. Starkey; Graham R. Hunt, who kindly performed laboratory spectrophotometric analyses of over 70 rock samples and answered many questions about rock spectra; and Leonard J. Schmitt, who discussed the geology of the area with the author.

The private sector has also been generous. Western Nuclear Corp. and the Lucky Mac Uranium Corp. kindly provided access to their respective properties at Crooks Gap. Roger Motten of Western Nuclear Corp. provided large scale maps of part of the field area and discussed the geology with the author. Steven Douglas of Western Nuclear Corp. and Charles D. (Don) Snow of Lucky Mac Uranium Corp. provided useful discussions in the field. Computer work at Stanford was performed on the STANSEARCH system, which is supported principally by gifts from Union Oil Corporation.

Finally the author wishes to express very special gratitude to his advisor at Stanford, Professor R. J. P. Lyon, whose continued guidance and criticism have improved the thesis and are greatly appreciated.

Although this thesis has benefited from the help of many, the content is solely the responsibility of the author.

This report was originally submitted as a thesis to the Department of Applied Earth Sciences and the Committee on Graduate Studies of Stanford University in partial fulfillment of the requirements for the degree of Master of Science.

Abstract

The Crooks Gap area is a major uranium producing district in south-central Wyoming. Uranium occurs there as roll-type deposits in Tertiary sandstones. Alteration of the host sandstones, related to the formation of the uranium deposits, is marked at the surface by a pronounced red coloration, which has long been used in the area as a prospecting guide. This report presents a characterization of alteration in the Crooks Gap area based upon (1) field observations of the extent and appearance of the alteration at the surface, (2) determination of the mineralogy and spectral reflectance characteristics of representative samples of altered and unaltered material in the laboratory, and (3) analysis of Landsat data of selected areas of altered and unaltered rocks.

Laboratory spectrophotometric data show that fresh, red-colored, altered rock has a strong absorption at 0.35 and 0.5 micrometers and a marked rise in reflectivity from 0.7 to 1.6 micrometers; weathered, red-colored, altered rock and Triassic red beds both show strong spectral absorption near 0.35 micrometers but have a relatively flat response from 0.7 to 1.6 micrometers. Landsat radiance values, simulated from the laboratory data, show that both altered rock and Triassic red beds are indicated by a high red-to-green ratio. This is in good agreement with actual satellite data over these rock types.

These data indicate that the Landsat system is very sensitive to ferric oxides and can map the distribution of these oxides in semiarid environments for reconnaissance purposes.

2. Introduction

This study began as a part of the Uranium Geophysics program of the U.S. Geological Survey. Crooks Gap, the southern Powder River Basin (both in Wyoming), and the south Texas coastal plain were areas that were chosen for study of the application of remote-sensing techniques to uranium exploration. These areas were chosen because in each case exposed alteration had been important in exploration for uranium ore and because the geology of the areas had been previously studied. The goal of the study was to determine if remote-sensing data could be used to discriminate alteration related to uranium ore deposits.

The author performed initial image processing of Landsat data of the Wyoming areas under the supervision of Terry W. Offield in 1975. Field work was carried out by Offield, Gary L. Raines, and the author in the summer of 1976 and by the author alone in August 1977. Initial results have been reported by Offield (1976). Laboratory mineralogical and spectral reflectance analysis of samples collected in the field (as well as additional image processing) was performed during the summer of 1977 at U.S. Geological Survey laboratories in Denver, Colorado, by the author.

Initially, image processing was aimed at producing an image product that best matched the mapped alteration patterns. However, it became apparent that the characteristics of the material types had to be better known from both satellite and laboratory data in order to decide how best to enhance the satellite imagery. A rationale was sought for processing of the data, to replace the initial hit-or-miss approach.

This paper presents the results of these studies for the Crooks Gap, Wyoming, area. Presentation of Landsat data in suitable image form was guided by field and laboratory studies and by analysis of the Landsat digital numbers.

The use of color terms, when applying to rocks, is strictly according to the "Rock Color Chart" of the Geological Society of America. Specifically, the term "red" is used here for the terms "pale to moderate red" (5R 6/2 to 5R 5/4) in the "Rock Color Chart."

3. Geology

3.1 Location and geography

Crooks Gap is located in Wyoming just south of the Granite Mountains and at the northern edge of the Great Divide Basin. Rawlins is 90 kilometers (km) to the southeast and Lander is 93 km to the northwest. The principal features of the Crooks Gap area are shown in figure 1.

The area slopes upward from an elevation of 1920 meters (m) at the Sweetwater River, to Crooks Gap at an elevation of 2010 m. This water gap, about 4 km wide, is flanked by Crooks Peak (elev. 2360 m) on the west and Sheep Mountain (elev. 2410 m) on the east. These erosional remnants are separated by low saddles from Crooks Mountain (elev. 2751 m) to the west, and Green Mountain (elev. 2751 m) to the east. A dissected surface slopes gently from Crooks Mountain to the south, but the south side of Green Mountain is marked by a prominent escarpment (Stephens, 1964).

The climate in the area is generally semiarid. Sagebrush and low grasses dominate the vegetation of the gap, but on Crooks Peak and Sheep Mountain scattered Limber Pines (Pinus flexilis) occur as well; these are replaced by forests of Lodgepole Pine (Pinus contorta var. murrayana) on the tops of Crooks and Green Mountains.

3.2 Previous work

The area has been studied extensively in the past, and the discussions on stratigraphy and structure presented here are largely drawn from the following published works. Stephens (1964) studied the geology and uranium deposits and mapped the immediate area at a scale of

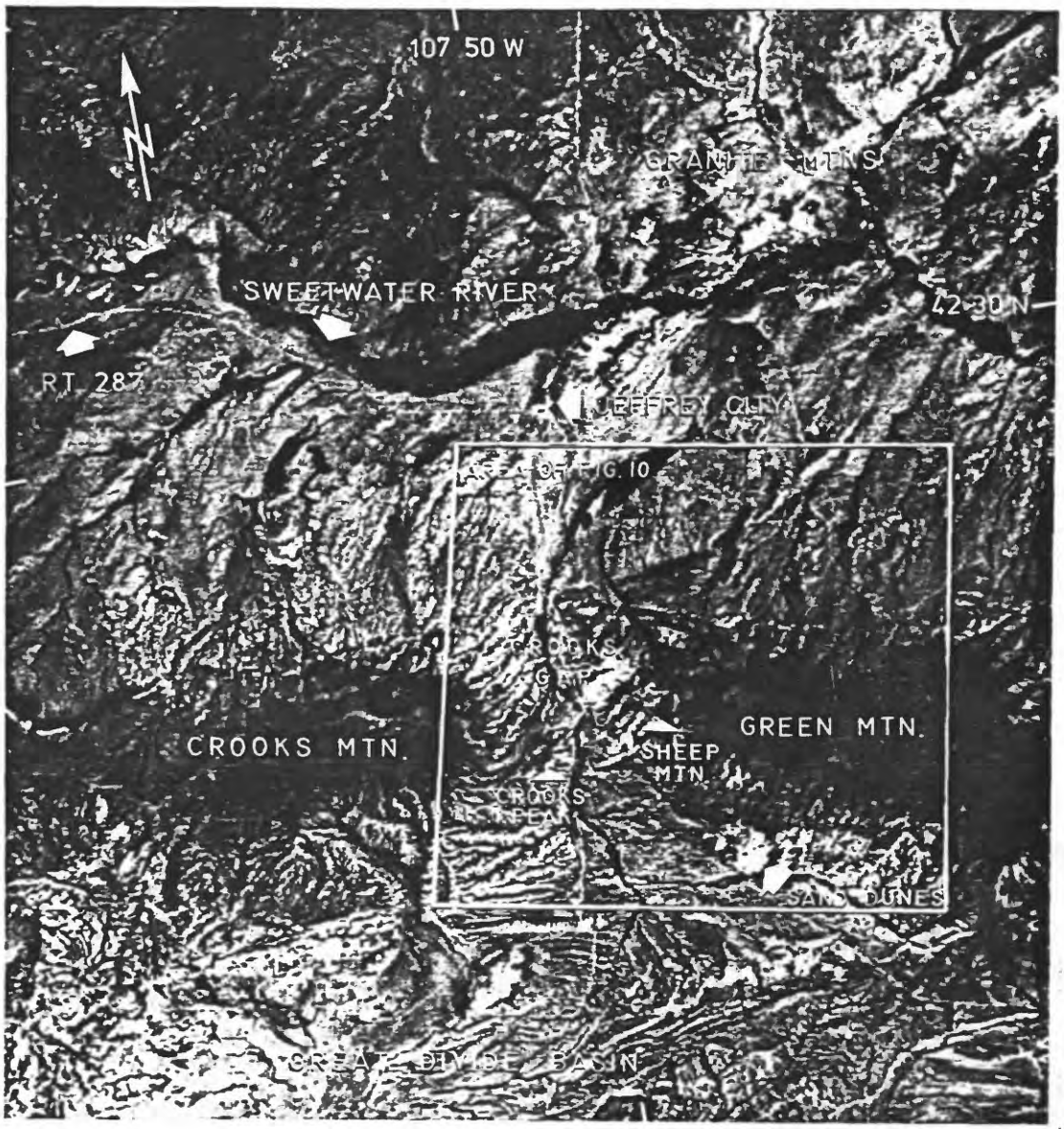

Figure 1.--Annotated Landsat image. Contrast-enhanced Landsat band 5 image of Crooks Gap, Wyoming. Scene ID is E-1409-17291 imaged on September 5, 1973, with a sun elevation of 47 degrees.

1:24,000 and surrounding area at 1:48,000. Love (1970) has studied the Cenozoic history of the Granite Mountains area and compiled a map at 1:125,000. Uranium occurrence and mining at Crooks Gap has been summarized in two review papers by Bailey (1969 and 1972). Files (1970) and DeNault (1974) have both discussed the uranium mineralization in the area. Most recently, Schmitt (1976 and 1977) has mapped the Sagebrush Park and Crooks Peak quadrangles at a scale of 1:24,000.

3.3 Stratigraphy

Rocks in the area range from Precambrian to Holocene in age. Inasmuch as the alteration related to uranium occurrence is restricted to the Eocene Battle Spring Formation, pre-Tertiary rock units are not discussed here but are summarized by Stephens (1964) and are discussed in detail by Keefer and Van Lieu (1966) and Pipringos (1968).

The Fort Union Formation of Paleocene age unconformably overlies the Cretaceous Cody Shale and is unconformably overlain by the Battle Spring Formation. The Fort Union is dominantly gray silty mudstone interbedded with thin units of carbonaceous shale, impure coal beds, and thin, lenticular, crosslaminated beds of sandstone. Iron-stained pebbles, iron staining of sandstone beds, and brown iron oxide staining is found throughout the formation. In addition, the unit contains pebbles of chert and silicified shale from the Cloverly and Mowry Formations. Clay-rich crusts develop over exposures of the Fort Union. The fine grain size of the rock and the carbonaceous material suggest deposition by sluggish aggrading streams on a broad flood plain.

The Battle Spring Formation of earliest Eocene age is herein discussed as defined by Love (1970) and is considered to be a northern facies of the Wasatch Formation. A complete description is given by Stephens (1964). The formation is largely conglomeratic arkose with interbedded cobble and boulder conglomerate and carbonaceous siltstone. The arkose is composed of poorly sorted, angular grains of quartz and partly weathered feldspar. Lenses of boulder conglomerate are common. The boulders are of a granite presumably derived from the Granite Mountains. The size of the boulder fragments increases upward in the section. Boulders and cobbles near the base of the unit, though, are derived from Paleozoic rocks. Higher in the section these materials are rare, and granite pebbles and cobbles predominate. This change in composition demonstrates a progressive erosion of nearby Paleozoic and then Precambrian rocks, resulting in a "reversed" stratigraphy (see Love, 1970, p. C35). The carbonaceous siltstone beds are lenticular, sandy, and poorly sorted. Carbonaceous fragments are abundant, but their distribution is erratic. The color of the unaltered rocks is a yellowish gray to pale greenish gray in fresh exposures, and somewhat more yellowish on weathered soil samples. In places, large rounded masses of a dark carbonaceous material with pyrite framboids indicate a highly reducing environment in the past.

The Crooks Gap Conglomerate (Battle Spring Formation member B of Stephens, 1964, and upper Battle Spring Formation of Schmitt, 1976) rests on the Battle Spring Formation and caps Crooks Peak and Crooks, Sheep, and Green Mountains. The formation consists of conglomeratic

arkose and giant boulder conglomerate. The rocks commonly have a reddish to orangish tint. The unit becomes finer grained toward the south, where it grades imperceptibly into the Battle Spring Formation. The origin of the unit is indicated as a deltaic fan extending southward from the uplifted Granite Mountains.

Younger rocks are exposed to the north of Crooks Gap. They are described in detail by Love (1970) and will not be discussed here.

3.4 Tectonics and structural history

The Crooks Gap area marks a major East-West structural boundary, consisting of complex faults and folds, with the Granite Mountains structural block to the north and the Great Divide Basin to the south. This boundary zone is characterized by anticlinally folded Paleozoic and Mesozoic rocks thrust over Cenozoic sediments. The boundary zone is delimited on the north by normal faults. North of these faults the remnants of a thrust sheet of granite are largely concealed by Eocene and later sediments (Stephens, 1964). The structural history presented here is from Stephens (1964) and Love (1970).

The period of Larmide tectonic activity (post-Late Cretaceous and pre-Paleocene in age) is represented by compression of Mesozoic and Paleozoic rocks into open symmetrical folds. Erosion of these folds is evidenced by silicified pebbles from the Mesozoic rocks found in the Fort Union Formation.

The Granite Mountains area was uplifted in early Eocene time, resulting in south-and southwest-moving thrust sheets. The lithology and structure of the Battle Spring Formation record the rapidity of

this uplift. Tectonic activity must have continued throughout most of the deposition of the formation because beds in it are strongly deformed, whereas beds in the overlying Crooks Gap Conglomerate are little disturbed; in addition, the Battle Spring Formation displays rapid facies changes. The presence of giant boulders in the Crooks Gap Conglomerate probably indicates that maximum activity of the Granite Mountains block occurred just prior to the deposition of the conglomerates. The boulders, then, record the subsequent rapid erosion of the thrust block.

The Granite Mountains block was buried by tuffaceous sediments in the late Tertiary. During and following this period the Kirk and East Kirk normal faults became active, resulting in downfaulting of the Granite Mountains block. North of Crooks Gap rocks of the upper part of the White River Formation, the Arikaree Formation and the upper part of the Ogallala Formation were deposited during early to middle Miocene time in a structural trough created by this downfaulting. Tuffaceous sediments of the Moonstone Formation, which accumulated in a lake that occupied this trough during early or middle Pliocene time after deposition of White River and Arikaree sediments, contain some beds unusually rich in uranium and are believed to be source rocks for part of the uranium present in the Gas Hills and Crooks Gap uranium districts (Love, 1970).

3.5 Uranium deposits and related host rock alteration

Uranium was first discovered at Crooks Gap in December 1953. As of 1972, 4350 metric tons of U_3O_8 had been mined. Currently (1977) the area is undergoing extensive exploration and development. Western

Nuclear Corp. operates at least six major shafts and one open pit in the area. The Lucky Mac Uranium Corp. has opened a new mine on the southwest flank of Green Mountain, just south of Crooks Gap. Drilling is being conducted on Green Mountain and to the immediate east in the Whiskey Peak area, where holes are being drilled to define an orebody.

The uranium occurs primarily as roll-type deposits in the Battle Spring Formation. In cross-section a roll is a crescentic area of mineralization in which the concave side encloses altered ground and the convex side points toward unaltered ground. In plan view, the lateral trace of the roll front is called the trend. The trend is usually sinuous, often joint controlled, and may be several kilometers long (DeNault, 1974). The area "enclosed" by the trend of the roll, in this case updip from the roll, is altered ground, and that downdip from the roll is unaltered ground. The alteration is not necessarily confined to a single stratigraphic horizon (Schmitt, 1976). The alteration is a result of the passage through the rock of oxygenating meteoric waters carrying uranium as a carbonate complex; roll fronts were formed where constituents such as pyrite or methane were in sufficient concentration to lower the Eh of the ground water (DeNault, 1974). Alteration recognized at the surface extends in a belt from the mine area in the gap southward and then eastward along the southern flank of Green Mountain to the Whiskey Peak area.

The alteration as exposed in surface outcrops may be separated into two main types: (1) red-colored, iron-stained alteration and (2) bleached alteration with no iron staining. Both are characterized by absence of

pyrite and carbonaceous material (which are commonly abundant in the unaltered rock) and by the alteration of feldspars to clay. In general the altered ground is clay-poor with respect to the unaltered ground. The red-colored alteration is a pale to medium red, and the bleached alteration is a yellowish gray to greenish gray.

The red-colored alteration occurs as lenses within the bleached alteration, generally concordant with bedding. Shapes vary, but the lenses are generally tabular and on the order of 10 cm to 2 meters in thickness. Sometimes these lenses are bound by thin clay layers; boundaries of these lenses may be controlled by grain-size differences, the staining occurring in the coarser material. The red-colored lenses represent at most about 20 percent of all altered material exposed on the surface, although to the eye, the red has a dominating effect and is thus used to delimit the alteration at the surface. The author concludes that this distribution of iron staining may be due to local high iron content of channels within the host rock; iron was oxidized in these channels by ground water, but not transported from them.

The occurrence of the red-colored alteration is different in conglomeratic facies than in arkosic facies. There are no lens-shaped areas of discoloration in the conglomerate; instead, boulders in the conglomerate are rimmed or capped by rinds of red staining of the matrix surrounding them.

4. Laboratory analysis of spectral characteristics

4.1 Justification

A significant part of this study was the investigation of spectral reflectance properties of bulk rock and soil material in the laboratory. Spectral reflectance measurements were supplemented with X-ray mineralogy as well as total-iron and ferrous-iron determinations. The object of this analysis was to provide a rationale for the processing and interpretation of Landsat digital data. To accomplish this, Landsat responses were simulated from the laboratory spectral reflectance data. This simulation allowed qualitative evaluation of the spectral character of the laboratory data in terms of Landsat spectral resolution, without the complicating factors of atmospheric scattering of the reflected radiation and low spatial resolution, which clumps reflectance from vegetation, rock, and soil into one measurement.

Laboratory spectral measurements set the limit for maximum possible spectral and spatial resolution--that is, the best discrimination of materials possible, based on spectral information. In addition, laboratory studies form a basis for intelligent processing and interpretation of remote-sensing data, because through the knowledge of specific spectral features, processing algorithms may be designed to specifically enhance these features.

Implicit to this justification is the assumption that the spectral features due to rocks and soil are the dominant contribution to the remote-sensing data signal. This study has not attempted to measure the effect of vegetation, surface roughness, and other nonmineral

related sources on the remote-sensing data, but it has attempted to assess their effect from the satellite imagery itself, rather than from ground measurements.

Significant mineralogical differences between altered and unaltered sandstones associated with similar uranium deposits in Wyoming and Texas that may be important for remote sensing are as follows:

1) Hunt (1977) points out that in the visible and near-infrared region, the most common spectral features are due to iron, water, or OH groups. Therefore, the iron and clay minerals are of utmost importance in this study.

2) Relative enrichment of ferrous-iron-bearing montmorillonites is reported in oxidized host rocks in the Shirley Basin by Harshman (1972). (Iron-bearing montmorillonites should show absorption at 0.97 micrometers. See Hunt, 1970.)

3) Depletion of total montmorillonite content in oxidized host rocks is reported in Texas by Daniels and others (1977).

4) Enrichment of Fe^{3+} is common in oxidized uranium host rocks. See, for example, Harshman (1974).

5) Kaolinization of feldspars in altered uranium host rocks is another common occurrence. See Dahl and Hagmaier (1974).

4.2 Sample collection

1) Samples were taken of surface covering generally representative of surface material in size range and color.

2) No attempt was made to orient the sample as it was being collected; rather, it was hand-scooped into a small sack.

3) Most surface samples were of soils developed from underlying bedrock, although in some areas the surface is contaminated with pebbles from erosion of overlying rock units, notably the Crooks Gap Conglomerate.

4.3 Sample analysis

1) Samples were examined under a binocular microscope for a first approximation of mineralogy.

2) A representative portion of the sample, excluding pebbles and cobbles, was crushed in a porcelain mortar to 200-mesh (75-micrometer) size. This was used for an X-ray powder mount of the whole sample for identification of minerals other than clays, such as alkali feldspar.

3) Laboratory spectrophotometric measurements were made by Graham R. Hunt using a Cary-14* spectrophotometer in the bidirectional reflectance mode (Hunt and Ross, 1967). This instrument has a variable slit width, but the spectral resolution is no worse than approximately one nanometer (G. R. Hunt, written communication, 1977). Calibration was performed before analyzing the samples by placing freshly prepared MgO in the sample holder and adjusting the reflectance over the 0.35 to 2.50 micrometer region to 100 percent as compared with the freshly prepared MgO internal standard. The instrument viewed a patch of the samples approximately one square centimeter in area. The samples were neither washed nor sorted.

4) The remaining sample was split three ways. One part went to the USGS analytical labs for determination of total iron and ferrous iron; total iron as Fe_2O_3 percent was determined by the atomic absorption method, and ferrous iron was determined by the potassium dichromate titration method. Another part was used for clay analysis, as described below, and the last part was saved.

4.4 Procedure for identification of clay minerals

1) The sample was emptied into a beaker partly full of water and agitated with an ultrasonic probe to loosen coatings and fine particles.

2) The suspension resulting was decanted and centrifuged immediately. After centrifuging for 6 minutes at 600 rpm, only particles two micrometers or smaller are left in suspension.

3) Oriented mounts for X-ray analysis are made by pipetting of the 2-micrometer suspension onto porcelain tiles.

* Use of brand names in this report is for descriptive purposes only and does not constitute endorsement by the U.S. Geological Survey.

4) For random orientation X-ray analysis, the suspension was decanted and water was removed with filter candles and by evaporating the rest of the water over a steam bath, leaving a powder.

5) X-ray analyses of a single sample were made with (1) untreated sample, (2) glycolated sample (to test for expandable clays), (3) sample heated to 400 degrees C, (4) sample heated to 550 degrees C (to separate clays from chlorites), and (5) powdered samples for random orientation run, when needed (emphasizes crystallographic orientations other than the (001) orientation).

6) The X-ray records were interpreted with assistance from Phoebe L. Hauff, Paul D. Blackmon, and Harry C. Starkey of the U.S. Geological Survey in Denver, Colorado. The percent of montmorillonite in the mixed layer clays was estimated where possible using a method described by Reynolds and Hower (1970).

7) Mineralogical analysis of samples is detailed in appendix 1 and summarized in table 2.

4.5 Discussion of laboratory spectra

The principal spectral features due to ferric iron oxides in the 0.4- to 2.5-micrometer region are demonstrated by the mineral hematite in figure 2. (Similar features are shown by goethite and limonite.) The spectral features of iron oxides are discussed in detail by Hunt and others (1971); the features that are of principal concern to this study are the strong absorptions 0.35, 0.5, and 0.85 micrometers. These features were well displayed by many samples from the Crooks Gap area.

A variety of spectral responses was shown by samples of the Battle Spring Formation. Spectra of representative samples are presented in figure 3. Red-colored altered samples all show strong absorption at approximately 0.35, 0.55, and 0.85 micrometers. Bleached altered samples show none of these features. Samples of red-colored altered

Table 2.--Summary of Laboratory Mineralogy

	Montmorillonite in mixed layer clays, percent	Total percent iron as Fe_2O_3	Iron-bearing phases
Battle Spring Formation			
Fresh red alteration	50-60	0.60-0.68	Fe-oxides
Weathered alteration	50-60	1.35-5.49	Fe-oxides
Bleached alteration	70-80	0.36	?
Unaltered	70-80	0.75-1.75	Pyrite
Red beds of the Chugwater Group	0	2.60-6.36	Hematite Fe-chlorite
Sand from dunes	0	0.28	Fe-oxides(?)

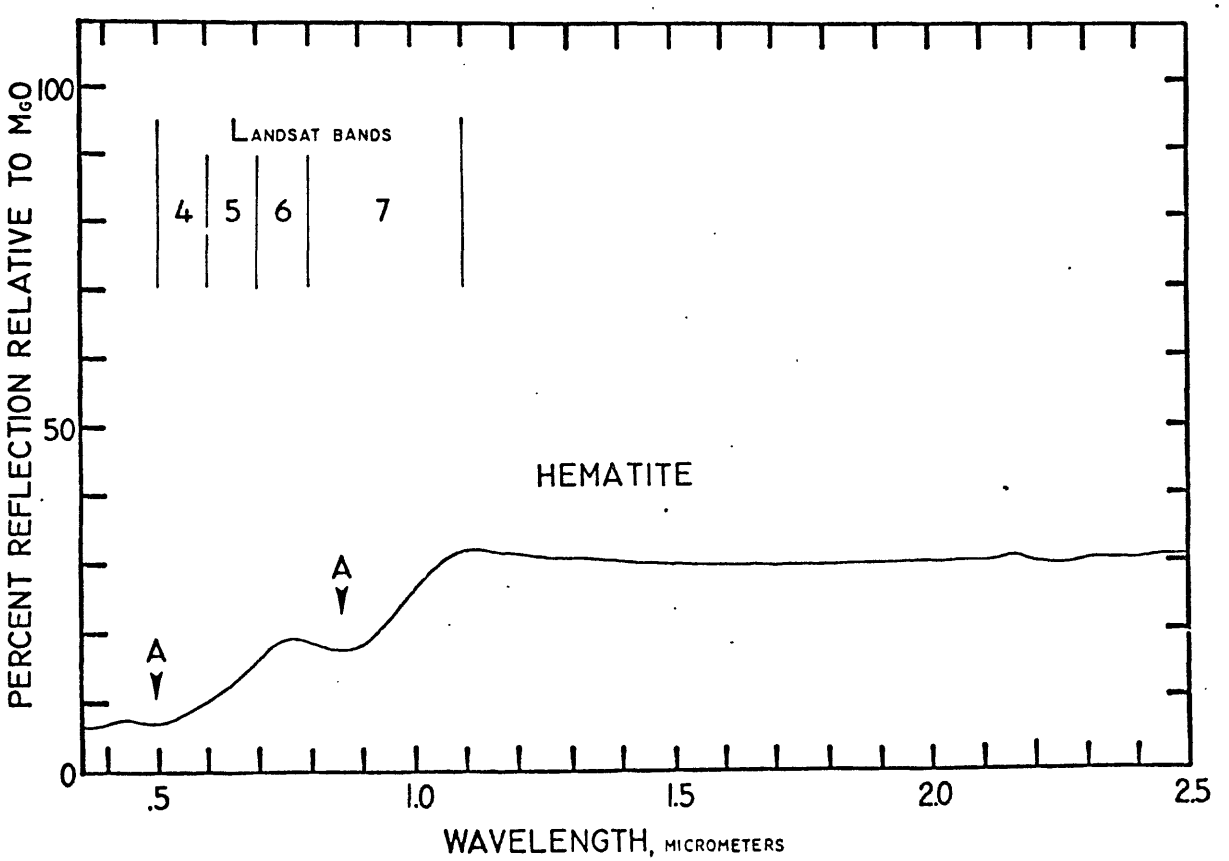

Figure 2.--Reflection spectrum of hematite. Redrafted from Hunt and others (1971). This spectrum is of a particulate sample in the 0-74 micrometer size range. The characteristic absorption features near 0.5 and 0.9 micrometers are indicated by the A's. This spectrum is representative of all iron oxide spectra published by Hunt and others, such as those for goethite and limonite.

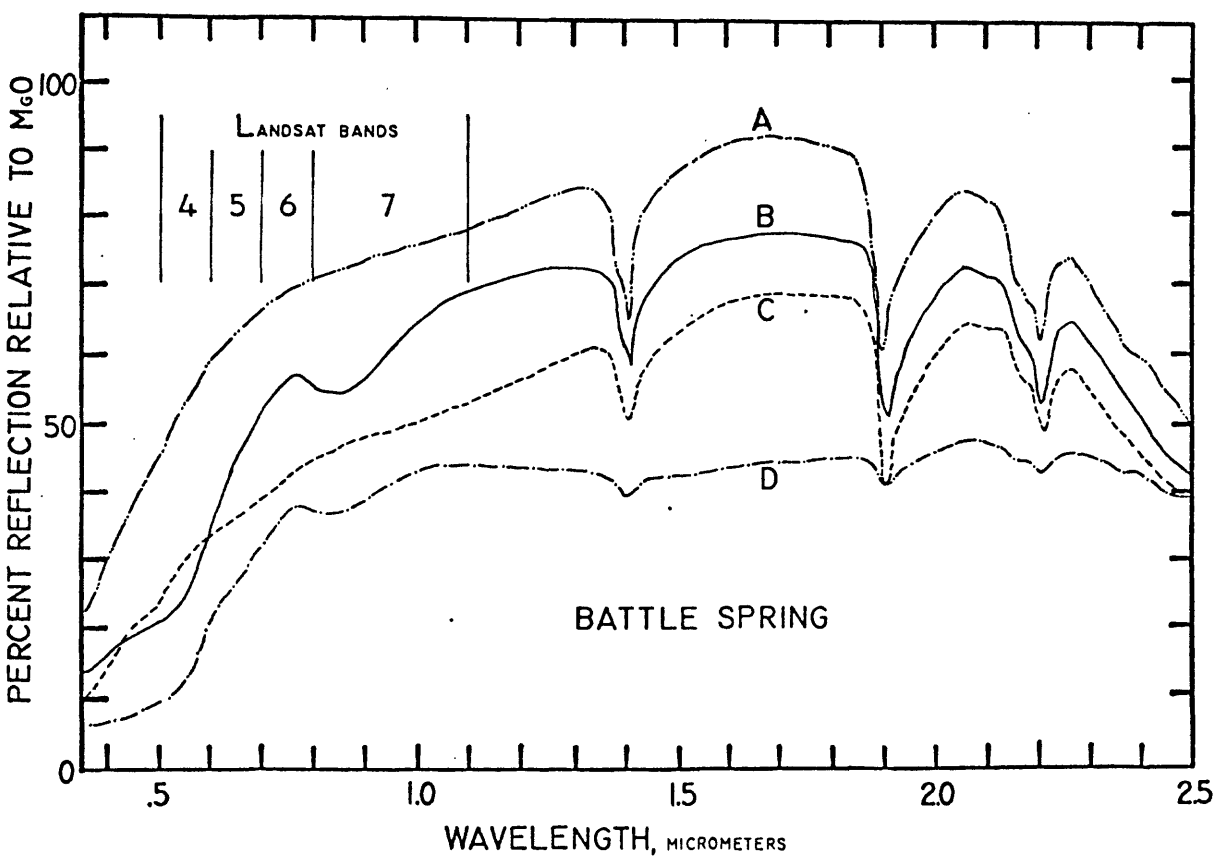

Figure 3.--Representative spectra of rocks of the Battle Spring Formation. (A) Bleached alteration sample CG77-11B; (B) fresh, pale-red alteration sample CG77-11R; (C) unaltered sample CG77-8; and (D) weathered red alteration sample CG77-5. Note the flatter spectral response of the weathered red alteration (D), compared to that of the fresh red alteration (B).

material that have been exposed to weathering in natural outcrop exhibit a flatter spectral response from 0.6 to 2.5 micrometers and have a less pronounced absorption feature at 0.85 micrometers than the freshly exposed red-colored altered material. Features due to iron absorption are generally weak or absent in the spectra of unaltered material. The relatively high percentage of total iron in these unaltered rocks is probably due to pyrite.

The samples of brownish-red rocks of the Chugwater Group (Triassic) also show spectral features due to ferric-iron absorption. Like the samples of the red-colored altered Battle Spring Formation, samples of the Chugwater Group show strong absorption at 0.35 micrometers and a sharp rise in reflectivity from 0.5 to 0.6 micrometers. At longer wavelengths, the Chugwater rocks are nearly spectrally flat, when compared with samples of freshly exposed red-colored altered Battle Spring Formation, which continue to show a strong rise in reflectivity to about 1.6 micrometers (see figure 4). The absorption feature at 0.85 micrometers is weak or absent in these rocks.

The broad 0.35- and 0.5-micrometer absorption feature due to iron oxides will be referred to in this report as the 0.5-micrometer absorption feature.

Mineralogy alone cannot adequately account for the suppression of the 0.85-micrometer absorption feature in the Triassic red beds, as the feature in either case is due to ferric oxide (G. R. Hunt, personal communication, 1977). The presence of hematite in the samples of the red beds is confirmed by X-ray analysis; although no identifiable

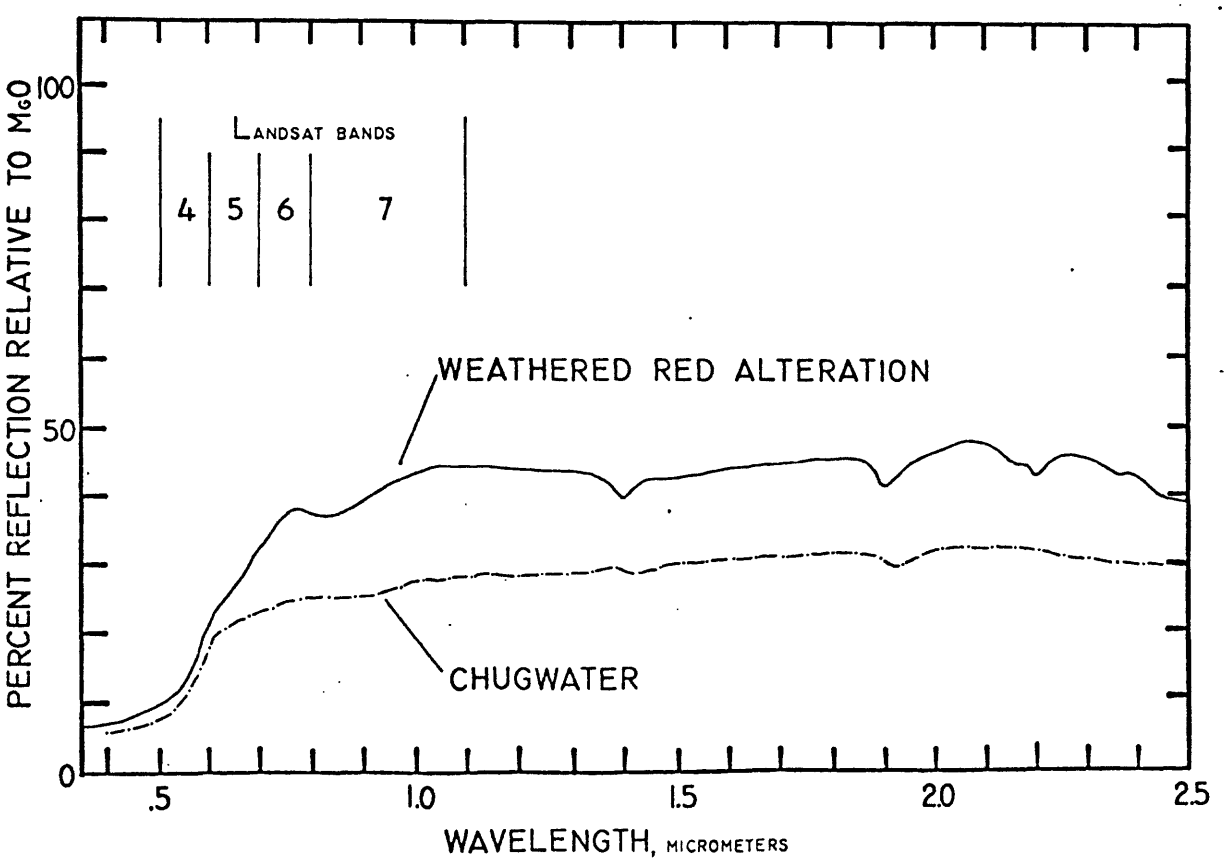

Figure 4.--Weathered red rocks. Weathered red alteration (sample CG77-5) is compared here with red rocks of the Chugwater Group (sample CG76-86).

hematitic peaks were observed in the analysis of the red altered material, the iron oxide in these samples is also very likely to be hematite. Observation of the centrifuged samples suggests that the iron oxide is evenly distributed among the size fractions in the samples of Triassic red beds of the Chugwater Group. However, in the samples of the fresh, red-colored altered rock from the Battle Spring Formation (notably in samples CG76-35 and CG77-1), the ferric iron oxide is primarily associated with silt-sized particles, because a moderate-red-colored portion settles out of suspension before the clays and after the silts, both of which are more light brown in color. While the spectra of the whole sample of this red-colored altered material show strong absorption at 0.85 micrometers, the light-brown clay-sized-particle separate shows only a weak feature at 0.85 micrometers and a much flatter spectral response. (See figure 5.)

Absorption features due to clays near 2.2 micrometers are observable in spectra for both altered and unaltered samples. (See, for example, the spectra of samples CG77-1 and CG77-8 in appendix 1 for comparison.)

Many samples from unaltered material, including unaltered Battle Spring Formation, mine dump samples, and samples from sand dunes, show slight but distinct absorption near 0.5 micrometers. Sand from the sand dunes (sample CG76-1) has a very slight coating of iron oxides, about 0.28 percent total iron expressed as percent Fe_2O_3; in hand-sample examination the sand appears a pale yellow to the eye. Samples of unaltered material frequently contain 1- to 2-cm pebbles of granite that have yellowish splotches, probably due to weathering of iron in

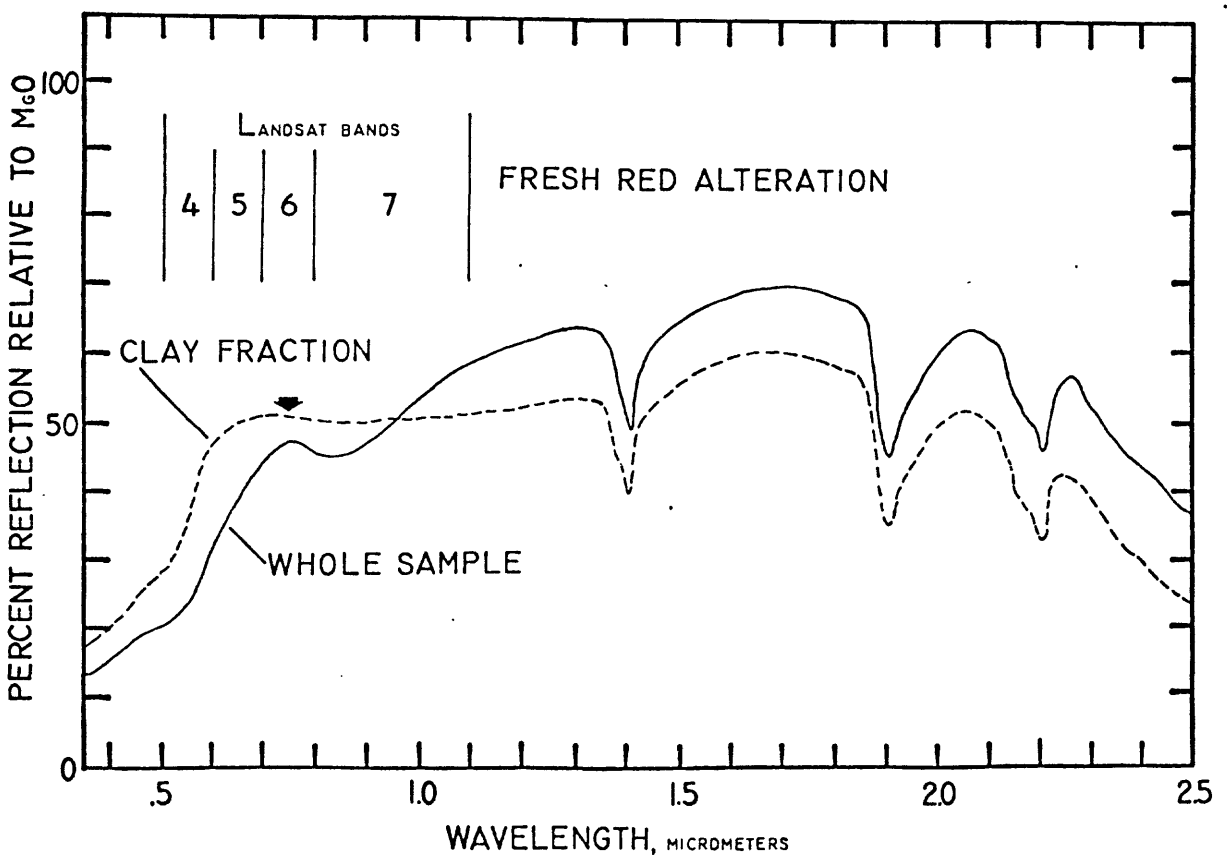

Figure 5.--Laboratory reflection spectra of clay size fraction (particles less than 2 micrometers) and of unsorted, unwashed whole sample with all size fractions (sample CG76-35 of fresh red alteration of the Battle Spring Formation). These are individual spectra and not averages. Note the flatter spectra and absence of the 0.75- to 0.85-micrometer peak (at the arrow) in the clay fraction.

the mafics. Spectral information derived from laboratory studies is summarized in table 1.

4.6 Summary of mineralogical studies

Important aspects of the mineralogy of the samples are detailed below. Table 2 provides a summary of the laboratory data.

1) No significant differences in species of clays were found in altered or unaltered host rocks. However, red-colored altered rocks have mixed-layer clays in which montmorillonite constitutes approximately 50-60 percent, and both unaltered rocks and bleached altered rocks have mixed-layer clays which consist of approximately 80 percent montmorillonite.

2) Iron oxides are ubiquitous, and even unaltered host and sand dunes exhibit some ferric oxide spectral absorption near 0.5 micrometers. Iron oxide staining is nevertheless far more pronounced in rocks that appear reddish.

3) Altered red-colored host rocks contain no iron-bearing silicates; iron oxide exists as ferric iron oxide coatings on detrital quartz, feldspar, and clay grains.

4.7 Simulation of Landsat data from laboratory spectra

Landsat data were simulated from the laboratory spectral measurements in order to characterize the reflectance spectra of the samples in terms of Landsat spectral resolution.

At this point it is necessary to explain some of the terminology associated with the Landsat digital data. The Landsat data this paper is concerned with come from an imaging device onboard the satellite called the multispectral scanner, or MSS for short. (See Rowan and others, 1974, for a more complete description of this spacecraft scanning system.) The MSS measures radiation in four regions or "bands" of the electromagentic spectrum. The composite MSS response in each

Table 1.--Summary of Laboratory Spectra
[Wavelengths in micrometers]

	Absorption		Reflectivity
	0.5	0.85	0.5 to 1.0
Battle Spring Formation			
Fresh red alteration	strong	strong	high
Weathered red alteration	strong	moderate	moderate
Bleached alteration	absent	absent	high
Unaltered	weak	absent	moderate
Red beds of the Chugwater Group	strong	weak	low
Sand from dunes	weak	absent	high

band is considered to be the product of the filter transmittance and the detector response of the instrument. The bands are named 4, 5, 6, and 7. Band 4 responds to radiation in the 0.5- to 0.6-micrometer region, band 5 to the 0.6 to 0.7 region, band 6 to the 0.7 to 0.8 region, and band 7 to the 0.8- to 1.1-micrometer region. The approximate response of these bands at 10-nanometer intervals is given in appendix 2 using graphical data supplied by W. Hovis (by a written communication, 1972, to R. J. P. Lyon) for an engineering model of the MSS system. Ratioing of these bands is used to gain a measure of the slope of the spectral response of a given material over several band widths. In this paper, ratios of bands are denoted as, for example, 5/4 meaning the ratio of band 5 (red light) to band 4 (green light).

The laboratory data (in the form of graphs on chart-paper output by the Cary-14 spectrophotometer) were digitized on a "graphics tablet" attached to a Tektronix TK4010 computer terminal. The result was a series of unevenly spaced points along the curve, which were input to a computer program that utilized a cubic spline method to interpolate values of reflectance at evenly spaced 10-nanometer intervals. The integrated response over a given band width was then calculated as the product of a given solar spectral irradiance, times the response of the MSS system and the target reflectance in the given wavelength interval, times 0.01 (the width of the intervals in micrometers), summed over the width of the band. This procedure produces a value in watts per square meter for the bandpass radiant exitance for the given band. The values used for solar spectral irradiance were taken from

the Air Force Cambridge Handbook of Geophysics (Valley, 1965) table 16-4 and are values of solar irradiance at sea level with an air mass of 2. The simulated Landsat data for the laboratory spectra are given in appendix 2 along with the values used for solar spectral irradiance and the Landsat band responses (essentially normalized filter transmittances). Figure 6 is a plot of the 5/4 versus 6/5 ratio values of the simulated Landsat data. The data are summarized in table 3, which includes means and standard deviations (in parentheses) of the "typical" rock types.

The samples in figure 6 are clearly separable into two groups based on the 5/4 ratio. One group with a 5/4 ratio less than 1.10 consists of dune sands, unaltered rocks and bleached altered rocks of the Battle Spring Formation, and mine dump samples; the other group, which has a 5/4 ratio greater than 1.0, consists of red-colored rocks of the altered Battle Spring Formation (including fresh and weathered samples), unaltered red beds of the Triassic Chugwater Group, and other unaltered but red rocks of Paleozoic age. In this second group, samples of the altered Battle Spring Formation show no separability from samples of unaltered but red rocks.

These data do not suggest separations of the samples based on the 6/5 ratio. The 5/4 ratio values range from 0.86 to 1.81, but the 6/5 ratio values have a much narrower range, from 0.91 to 1.17. Based on these laboratory data, large variations (with respect to the variations shown by the 5/4 ratio values) in the 6/5 ratio values of actual satellite data are probably not due to the rock/soil spectral reflectance properties of these "typical" materials.

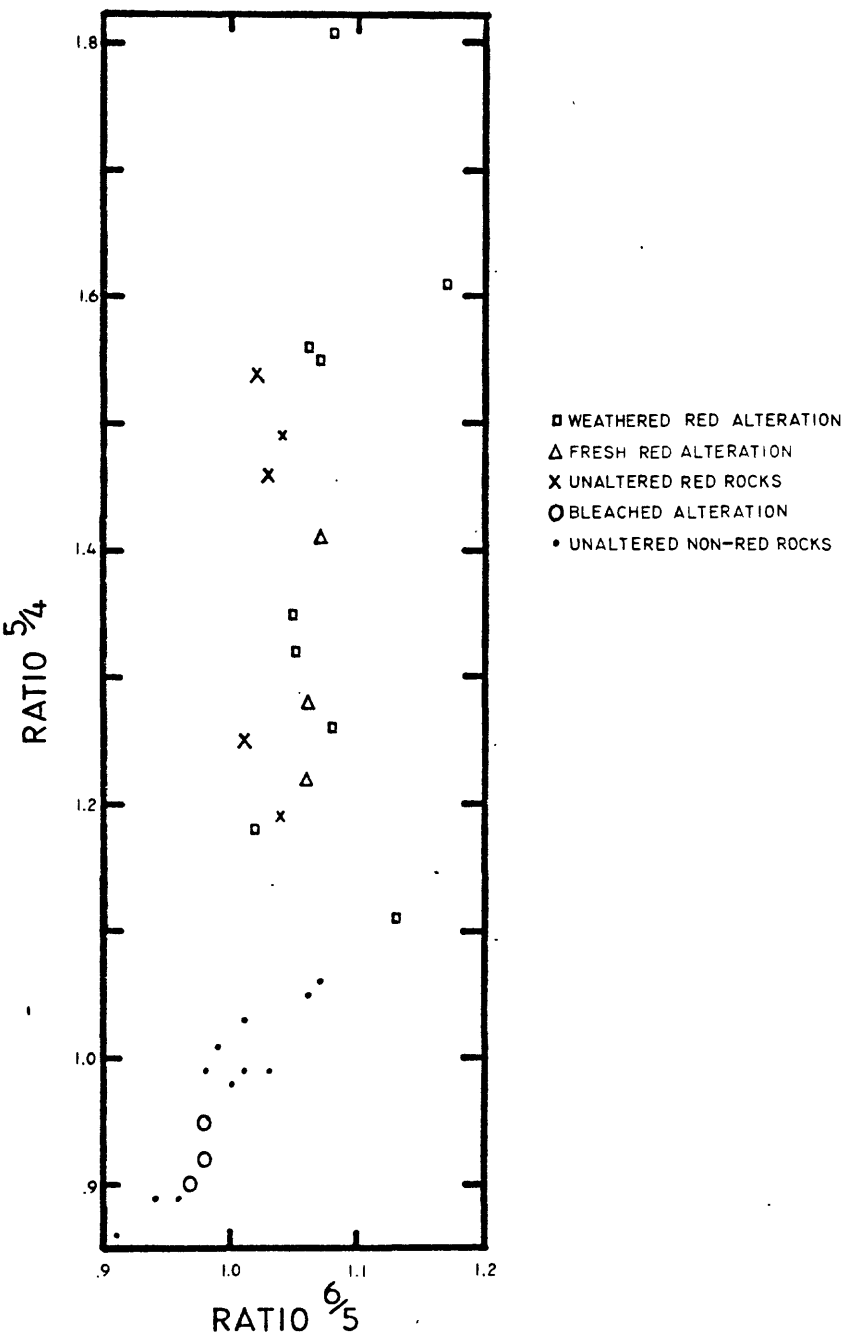

Figure 6.--Simulated Landsat data. A plot of the 5/4 versus the 6/5 ratio values for the laboratory samples. Each symbol represents a single measurement. Note that red rocks vary largely as a function of 5/4 only, but that non-red rocks vary as a function of both 5/4 and 6/5.

Table 3.--Simulated Landsat Data
[Landsat band data given as radiant exitance in watts per square meter]

	Altered rocks			Unaltered rocks	
	Fresh red (N=3)	Weathered red (N=9)	Bleached red (N=3)	Red (N=5)	Other colors (N=10)
Band 4	28.90 (1.34)	17.75 (4.73)	55.31 (4.68)	16.90 (3.91)	33.48 (6.22)
Band 5	37.68 (3.59)	24.46 (5.00)	50.99 (5.52)	23.03 (3.53)	32.78 (7.20)
Band 6	40.06 (4.06)	26.36 (5.12)	49.69 (5.44)	23.64 (3.51)	32.87 (7.98)
Band 7	54.82 (5.98)	38.09 (7.38)	69.83 (7.19)	34.01 (5.46)	47.80 (11.59)
Ratio 5/4	1.30 (0.10)	1.42 (0.23)	0.92 (0.03)	1.39 (0.16)	0.98 (0.07)
Ratio 6/5	1.06 (0.10)	1.08 (0.05)	0.98 (0.01)	1.03 (0.01)	1.00 (0.05)
Ratio 7/5	1.46 (0.03)	1.56 (0.11)	1.37 (0.01)	1.48 (0.04)	1.45 (0.12)
Ratio 7/6	1.37 (0.02)	1.44 (0.08)	1.41 (0.01)	1.43 (0.03)	1.46 (0.05)

Means and standard deviations (in parentheses) for bands and ratios of a given rock type.

5. Analysis of Landsat data

5.1 Approach

The objective of this study was to evaluate the usefulness of the Landsat data in identifying the alteration related to the uranium deposits at Crooks Gap. Thus far the spectral and mineralogical properties of selected rock and soil samples from the area have been determined, and Landsat radiance values have been simulated from these data. These simulated data provide a basis for interpretation of the actual satellite data. This section is divided into three parts. The first part presents the characteristics of various rock and soil types as depicted in the Landsat data. These data are then compared with the laboratory simulated Landsat data. The second part examines the effect on the satellite data of atmospheric scattering and how this may account for discrepancies between the laboratory data and the satellite data. The preceding analysis was used in the third part to constrain the interpretation of a digitally enhanced Landsat image of the Crooks Gap area. The image was compared with a geologic map to assess the significance of the spatial information in the image.

5.2 Characterization of Landsat data

Eight ground sites of approximately 7 to 42 acres each were chosen as being representative of either altered rock, unaltered rock, or vegetation in the area. These sites were chosen for uniformity of vegetation and mineralization as estimated by ground observation. The pixel values for these sites were then extracted for analysis using the STANSORT computer programs. (See Honey and others, 1974.) Statistics

of the Landsat data for scene 1013-17300 of August 5, 1972, and brief descriptions of the sites are given in appendix 3. These data are summarized in table 4. The important characteristics of the data are as follows:

1) Sites dominated by red-colored rocks of the altered Battle Spring Formation or red-colored rocks of the unaltered Chugwater Group are both characterized by 5/4 ratio values greater than 1.15.

2) Sites dominated by vegetation have a low 5/4 ratio and a high 6/5 ratio.

3) The sand dunes display a 5/4 ratio value that is nearly as high as that of red rocks, but in the laboratory data, sand from this locality showed a low 5/4 ratio relative to red rocks. The anomalously high 5/4 ratio value in the Landsat data may be due to atmospheric effects, which will be examined in the next section.

The break in the 5/4 ratio between red rocks and non-red rocks is nearly the same for both the laboratory data and the satellite data. This break has been found in Landsat data for many other areas as well (see Lyon, 1977). Rocks with a 5/4 ratio greater than 1.10 to 1.15 all show significant ferric iron absorption, which is weak or absent in rocks with a 5/4 ratio less than 1.10 to 1.15 (compare tables 3 and 4).

Published laboratory spectra for selected desert plants have a marked rise in reflectivity near 0.7 micrometers (Gates and others, 1965), as shown in figure 7. Landsat data simulated from these spectra are as follows:

Table 4.--Landsat Data Summary

[Data used are uncorrected Landsat radiance values (raw DN values). Site letter designations refer to locations shown in figure 10. The Landsat scene ID is E-1013-17300, imaged on August 5, 1972, with the sun at an elevation of 55 degrees and an azimuth of 128 degrees. Vegetation density was estimated from ground observations. The mean band radiance is the average of the four uncorrected bands in units of raw DN (digital number). Landsat band 7 is multiplied by 2.]

Site	Description	Vegetation density	Ratio 5/4	Ratio 6/5	Mean band radiance
(A)	Fresh red alteration	low	1.317	1.040	74.20
(M)	Weathered red alteration	low	1.253	1.089	56.24
(C)	Red beds of the Chugwater Group	low	1.270	1.064	45.87
(U)	Unaltered Battle Spring Formation	moderate	1.112	1.051	43.00
(T)	Mine dump	none	1.118	0.934	79.10
(S)	Sagebrush field	high	1.100	1.134	41.19
(G)	Pine forest	high	0.803	1.748	24.17
(D)	Sand dunes	low	1.222	1.032	91.47

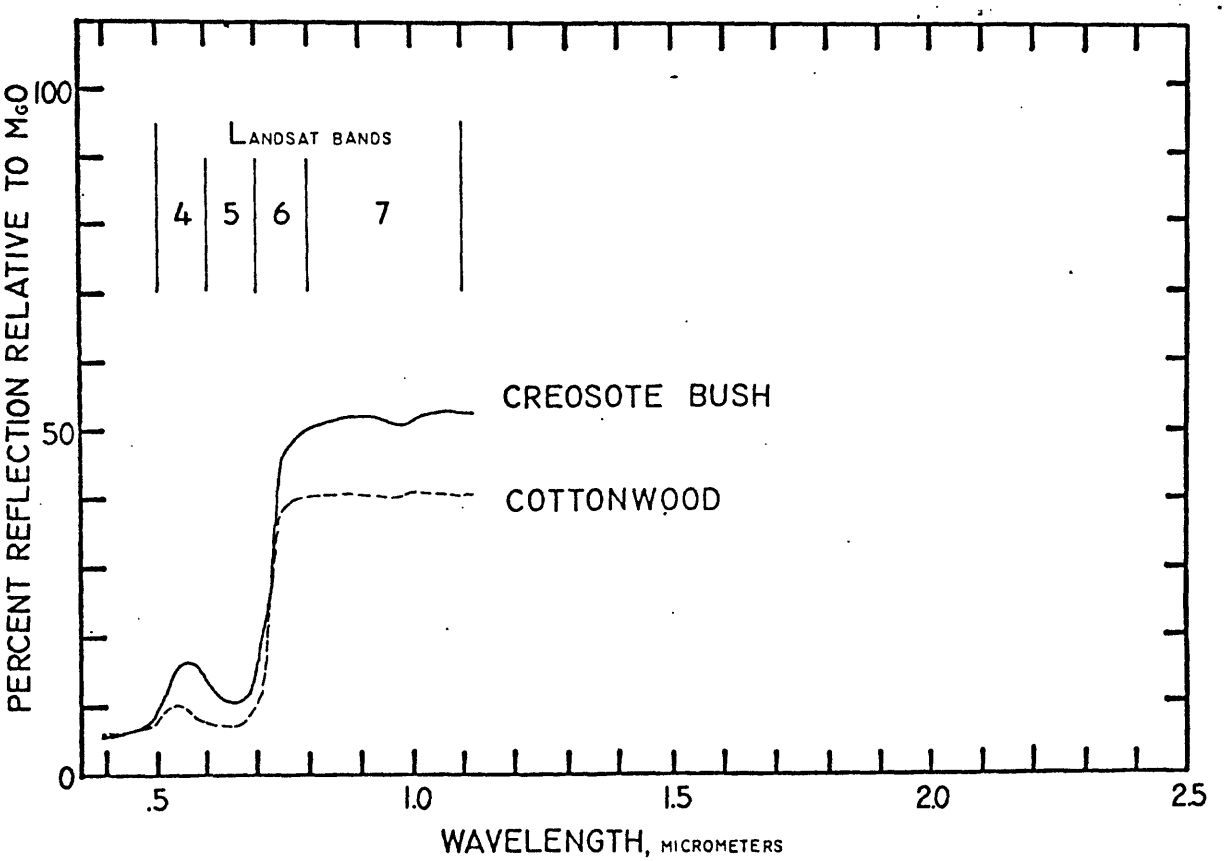

Figure 7.--Spectra of desert plants. These spectra have been redrafted from Gates and others (1965). Solid line represents laboratory spectra of stems and leaves of Larrea divaricata, the creosote bush (Gates, fig. 4a); and dashed line shows reflectance of the upper surface of a leaf of Populus deltoides, a cottonwood (Gates, fig. 2a). Note the sharp rise in reflectivity near 0.7 micrometers.

Landsat Band	4	5	6	7	5/4	6/5
Cottonwood leaves	9.13	6.87	23.47	42.75	0.753	3.414
Creosote bush	15.21	10.63	24.98	54.03	0.699	2.828

These data have 6/5 ratio values considerably greater than any of the laboratory samples of rock or soil, due principally to the sharp rise in reflectivity of the vegetation near 0.7 micrometers. Sites in the Landsat data dominated by vegetation show a high 6/5 ratio value as well, whereas sites where vegetation is scarce show a much lower 6/5 ratio. The satellite data coupled with the ground observations suggest that the 6/5 ratio varies largely according to vegetation. The laboratory data further suggest that the 6/5 ratio varies relatively little according to rock and soil types. Although the laboratory spectra of plants given here may not be representative of those at Crooks Gap, nevertheless, they demonstrate that the sharp rise in reflectivity of vegetation near 0.7 micrometers results in a high 6/5 ratio value.

5.3 Effects of atmospheric scattering

The effect of atmospheric path radiance on the signal perceived by the Landsat satellite was discussed by Rowan and others (1977). They demonstrate that this path radiance term is much more important for dark targets than light targets. That is, although the added radiance is the same for each target, it is nearly as great as the total radiance of a dark target. Thus, after subtraction of the added radiance, the band radiance values are small, and ratios resulting from these "corrected" bands are more sensitive to the variance in the data.

An atmospheric scattering correction was applied to Landsat scene E-1013-17300 in order to see how the ratio values for various light and dark targets would be affected. The correction values used were the minimum DN values (minus one) of the 256 by 256 pixel subarea of the Landsat scene centering around Crooks Gap. This "minimum radiance" was assumed to be the atmospheric scattering component. Statistics of selected sites at Crooks Gap have been given previously in section 5.2. The correction was applied by subtracting these minimum radiance values from each pixel in the scene, band for band (although only bands 4 and 5 were corrected in this case); statistics were then acquired for selected sites. The percent difference between the ratios of "corrected" and uncorrected data was then calculated for ratio 5/4 and plotted in figure 8. The data are given in table 5. The results agree in general with figure 6 of Rowan and others (1977). The ratio values for the corrected data show a significant difference between the sand dunes (D) and the dark red beds (C), but the difference was not significant for the uncorrected data. Because the sand dunes are bright, the correction has less of an effect on the 5/4 ratio of sand dunes than on the 5/4 ratio of the dark red beds of the Chugwater Group. The resulting ratios are easily separable, as the laboratory data of the sand suggests, although the red to non-red break is no longer near 1.10 to 1.15.

Correction for atmospheric scattering by making a "dark-target" subtraction may introduce considerable error into the ratios because of the variance of the data (both the dark subtraction value and the data to be corrected). For this reason, no atmospheric correction has been

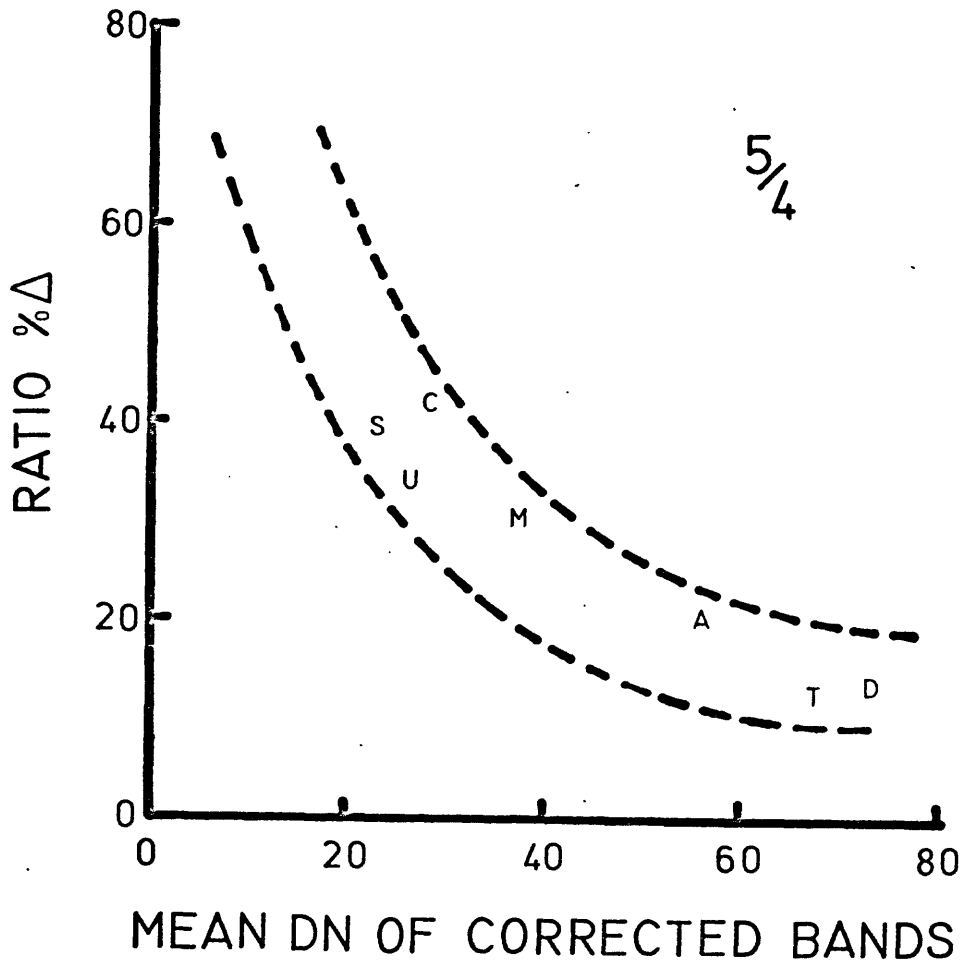

Figure 8.--Effects of atmospheric correction. The percent difference between corrected and uncorrected 5/4 ratios is given as a function of average spectral reflectance of the corrected bands 4 and 5. The data show that the ratio values of dark objects change more than do the values for bright objects upon dark-object subtraction. The letters refer to the following sites given in figure 10, (A) fresh red alteration in the Snobal open pit, (M) weathered red alteration in the mining area, (C) Chugwater Group red beds, (U) unaltered Battle Spring Formation, (T) dump of Seismic open-pit mine, (S) dense sagebrush on Greet Mountain, and (D) sand dunes.

Table 5.--Atmospheric Correction Values

	Site	Corrected average 4 + 5	Uncorrected ratio 5/4	Corrected ratio 5/4	Ratio % Δ
(A)	Fresh red alteration	55.92	1.317	1.593	20.9
(M)	Red weathered alteration	37.26	1.253	1.633	30.3
(C)	Red beds of the Chugwater Group	28.39	1.270	1.812	42.7
(U)	Unaltered Battle Spring Formation	36.41	1.112	1.496	34.5
(T)	Mine dump	67.89	1.118	1.255	12.3
(S)	Sagebrush field	22.90	1.100	1.538	39.8
(G)	Pine forest	3.20	0.803	2.039	153.9
(D)	Sand dunes	73.07	1.222	1.387	13.5

Correction values used were: band 4 = 18, band 5 = 12.

made in subsequent image processing. Ambiguities such as the anomalously high 5/4 ratio values of the sand dunes (as compared to other unaltered materials; see table 5) may be recognized by the interpreter of the data by using single-band imagery to match bright objects with 5/4 ratio anomalies. Note that the correction has had the effect of increasing the 5/4 ratio values of dark, non-red targets, such as the sagebrush field and the pine forest sites, so that they bracket the values of the red targets. (See table 5.) Hence, the red and non-red targets are no longer separable.

5.4 Image display

One of the most useful ways of examining Landsat data is in image format. In this form the data may be spatially compared with geologic maps and other map-based data. The image is also a form familiar to the photo-interpreter. It has been shown previously that a color composite of band ratios (called a color-ratio composite or CRC) displays information that is not displayed by single bands or combinations of single bands (Rowan and others, 1974). Furthermore, it has been shown in the previous sections of this report that the 5/4 ratio is sensitive to ferric iron absorption and that the 6/5 ratio is sensitive to vegetation, two factors that may be of use in exploration in the Crooks Gap area.

A color-ratio composite (CRC) was prepared for the Crooks Gap area in the U.S. Geological Survey laboratories in Denver, Colorado, in September 1977 using the procedure of Rowan and others (1974). In addition, to further enhance the 5/4 ratio, only ratio values greater than 1.20

were stretched into the dynamic range of the display, saturating all lower ratio values to zero density (no film darkening). Processing of the image was complete before the analysis of the Landsat data at Stanford University. Therefore, input from the analysis of the Landsat data to the construction of the CRC did not take place, but the analysis has been useful in the interpretation of the CRC.

The procedure of Rowan and others (1974) for construction of the CRC results in a sandwich of positive Diazo copies of three ratio images: ratio 4/5 copied in cyan (minus red), ratio 5/6 copied in yellow (minus blue), and ratio 6/7 copies in magenta (minus green). Analysis at Stanford has employed the inverse ratios 5/4, 6/5, and 7/6. For consistency with the previous sections of this report, the ratios of the CRC will be discussed as 5/4, 6/5, and 7/6 with the relative ratio values inverted, since the two representations are the inverse of each other. Hence a "low" 4/5 ratio value is a "high" 5/4 ratio value. The film for each ratio image was exposed so that a greater density (darker film) is related to, for example, a high 5/4 (or a low 4/5 ratio value). A Diazo copy of this image is colored where the original ratio image was darkened, and clear where the original was clear. Therefore, if the 5/4 ratio was copied in cyan, then a saturated shade of cyan represents a high 5/4 ratio value when compared with a less saturated shade of cyan, which would have a smaller 5/4 ratio value. These relations and the resulting combinations of these subtractive colors are summarized in table 6. To repeat, although the ratio images were based on the ratios 4/5, 5/6, and 6/7, the discussion here refers to the

Table 6.--CRC Colors

Component colors	Colors resulting from the indicated combinations		
	"Red" (orange)	Green	Blue
5/4 Copied in cyan (minus red)		x	x
6/5 Copied in yellow (minus blue)	x	x	
7/6 Copied in magneta (minus green)	x		x

inverted ratios 5/4, 6/5, and 7/6. The following is a summary of important characteristics displayed by the CRC (fig. 10).

1) Vegation is depicted by orange, which results from relatively high ratio values of both 6/5 and 7/6; note especially Green Mountain, the top of which is covered by lodgepole pine, as at G. (See figs. 9 and 10.)

2) Most of the area is covered to some extent by sagebrush, hence most of the area shows an orange color.

3) Greens and blues are combinations of relatively high 5/4 ratio values with either 6/5 for green, or 7/6 for blue. Ground observations suggest that the blue indicates exposed ferric iron oxides with little or no vegetation, and the green indicates exposed ferric iron oxides with low density vegetation. Sand dunes (D) with relatively small amounts of ferric iron oxides are blue and green in the CRC not because of mineralogy, but because of the brightness of the dunes and atmospheric scattering, as discussed previously.

4) Scattered pixels of blue and green occur throughout the image. In the northern half of the image many of these occur in drainages and may represent products of erosion of the Paleozoic red beds. In the southern half the blue and green pixels are more uniformly scattered and probably show the weathering of mafic minerals of granitic fragments in the arkosic Battle Spring Formation, though they may result from high brightnesses like those associated with the sand dunes.

5) In the immediate area of Crooks Gap, the distributions of altered rocks at M and Triassic red beds at C (refer to figs. 9 and 10) are well delineated by the CRC. Areas of altered Battle Spring Formation on the south flank of Green Mountain, as mapped by Schmitt (1976), are not shown by the CRC primarily because of the abundant vegetation, an extensive covering of soil in most places, and lack of good exposures. It is possible, however, to trace the Triassic red beds along the northern edge of Green Mountain in approximate coincidence with the East Kirk Normal Fault.

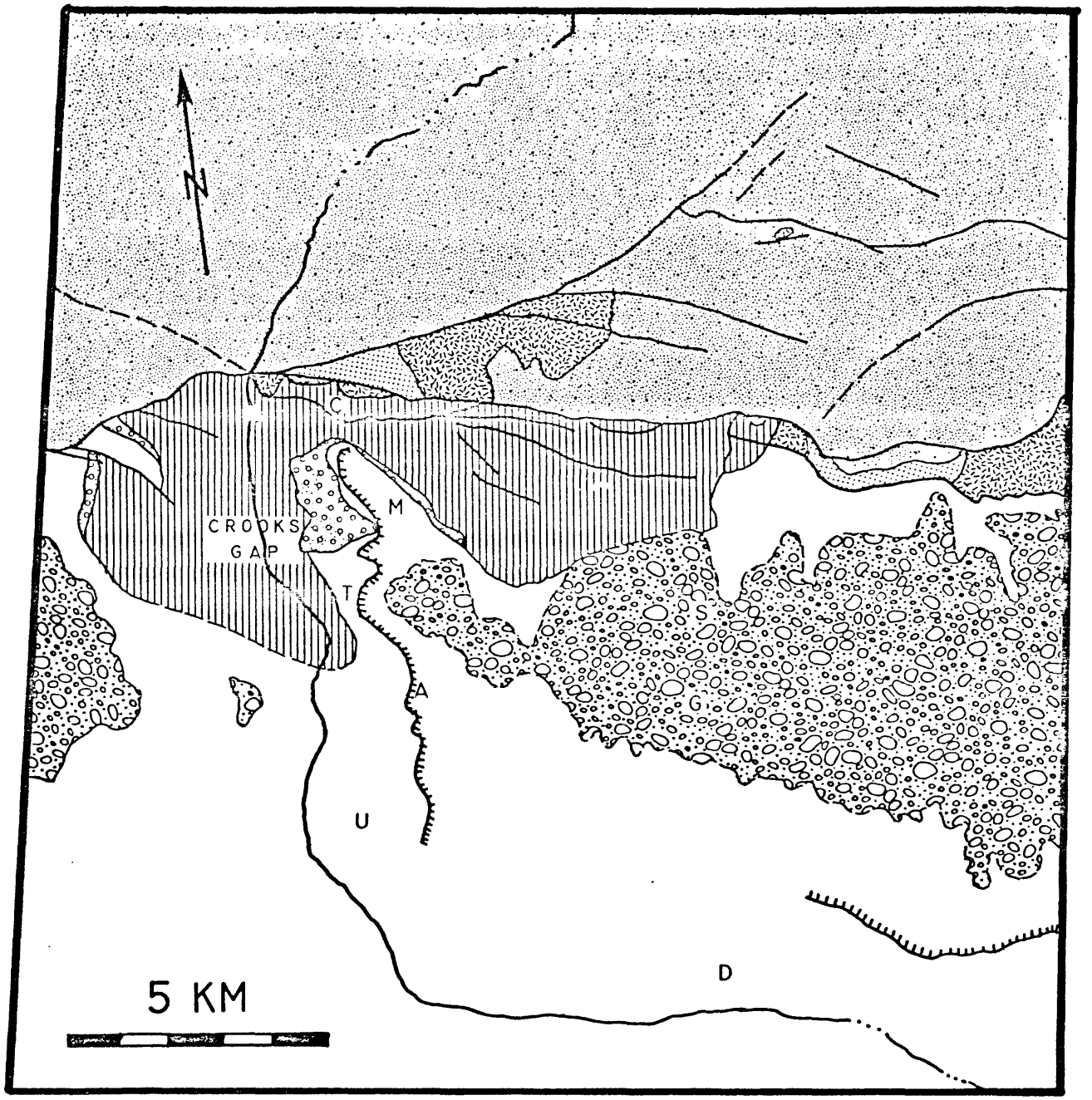

Figure 9.--Geologic map of the area shown in figure 10. (See following page for explanation.) Lettered sites are (A) fresh red alteration in the Snobal open pit, (M) weathered red alteration in the mining area, (C) Chugwater Group red beds, (U) unaltered Battle Spring Formation, (T) dump of Seismic open pit mine, (S) dense sagebrush on Green Mountain, (D) sand dunes, and (G) alteration boundary from Schmitt (1976 and 1977) and field mapping by the author in 1977. Map compiled from Love (1970).

Explanation

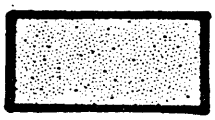

Miocene rocks (Ogallala Formation, lower part; Arikaree Formation; White River Formation, upper part)

Tuffaceous, grayish-pink, fine- to medium-grained sandstone.

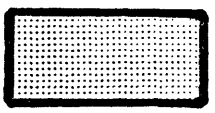

Upper to middle Eocene Wagon Bed Formation

Very tuffaceous claystone, siltstone, and sandstone; green, yellow, and olive drab to gray.

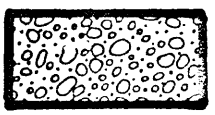

Middle to lower Eocene Crooks Gap Conglomerate

Giant boulders of Precambrian rocks in a gray to pink arkosic sandstone matrix.

Lower Eocene Wasatch and Battle Spring Formations, undivided

Interbedded gray arkosic sandstone with brown and red iron staining.

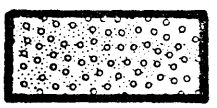

Paleocene Fort Union Formation

Predominantly silty mudstone interbedded with thin units of carbonaceous shale, impure coal beds, and lenticular, cross-laminated beds of sandstone.

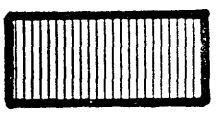

Mesozoic and Paleozoic rocks

Includes gray Cretaceous Cody Shale, Triassic Chugwater Group with red shales, and Mississipian and Cambrian sediments.

Precambrian igneous and metamorphic rocks

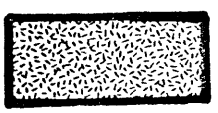

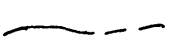

Contact. Dashed where approximately located.

Fault. Dashed where approximately located, dotted where concealed.

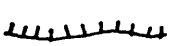

Alteration boundary. Approximate lowest stratigraphic limit of red supergene oxidative alteration. Hachured on side of boundary with indicated alteration.

Figure 10. (Next page.)--Three-component color-ratio composite (CRC) of the Crooks Gap uranium district, Wyoming (scale of 1:125,000), made from diazo-color separates, showing areas of ferric-iron absorption in green and blue,* and vegetation in orange. Landsat scene ID is E-1409-17291, imaged on September 5, 1973, with a sun elevation of 47 degrees.

*Note.--Copies of this photo made by color-copying machines may show the green and blue areas as black or dark purple. Prints of this photo are available for inspection at U.S. Geological Survey libraries in Reston, Va., Denver, Colo., and Salt Lake City, Utah; and at the library of the Wyoming Geological Survey in Laramie.

6. Summary and conclusions

Alteration of the arkose of the Eocene Battle Spring Formation is exposed at the surface by mining activities and by natural outcrops in the Crooks Gap area. The altered arkose is characterized by the removal of mafic minerals and the kaolinization of feldspars. Thus, most of the alteration has a white or bleached appearance. Occurring within this bleached arkose are local bodies of pale-red-colored altered arkose. This red-colored alteration makes up less than 20 percent of the outcrop of the altered rock, but it is the chief criterion by which it is recognized. Localization of the red coloration probably resulted from in-situ oxidation of silt-sized pyrite grains by the oxidizing ground water. The red-colored altered arkoses contain less than one percent total iron (expressed as percent Fe_2O_3).

The Triassic Chugwater Group, the shales of which are a brownish-red, crop out prominently at Crooks Gap. These rocks contain up to 6 percent total iron, mostly as hematite.

The freshly exposed pale-red-colored altered rocks probably contain ferric iron oxides, after pyrite, associated with the silt-sized particle fraction. The laboratory spectra of these rocks show particularly strong absorption near 0.5 micrometers, a strong absorption feature at 0.85 micrometers, and a sharp rise in reflectivity from 0.5 to 1.7 micrometers. Surficial weathering of these rocks would tend to redistribute the iron as a coating on other particles of all size fractions. The spectra of such material show a less reflective, generally flat response from 0.7 to 2.5 micrometers, with a strong absorption at 0.5 micrometers.

The spectra of this weathered alteration are similar to spectra of red shales of the Chugwater Group, which also exhibit a strong absorption at 0.5 micrometers with a generally flat spectral response from 0.7 to 2.5 micrometers. Unaltered rocks and white or bleached altered rocks of the Battle Spring Formation show no absorption features due to ferric iron oxides.

The mineralogy of the samples was studied using X-ray diffraction. These analyses indicate that the altered rocks do not contain iron-bearing silicates, and so the ferric-iron absorption features shown by these samples are probably due to coatings of ferric iron oxides. Also, there is no significant difference in species of clays between altered rocks and unaltered rocks.

Landsat radiance data were extracted for sites dominated by altered and unaltered rocks and vegetation. Red-colored altered rocks of the Battle Spring Formation and Chugwater Group are characterized by high 5/4 ratio values. An interpreter may very easily distinguish Chugwater Group rocks from the altered rocks with the aid of geologic maps. Vegetation is characterized by low 5/4 and high 6/5 ratio values. The sand dunes show a high 5/4 ratio value, despite a very low total iron percentage, because of their high reflectivity and atmospheric scattering.

From an exploration standpoint, these data indicate that discrimination of Triassic red beds and weathered, altered arkoses may not be possible based on spectral information alone; however, the Landsat system is very sensitive to exposed ferric iron oxides and may be used to map

them for reconnaissance purposes. Suitably processed Landsat imagery coupled with geologic maps and other data bases may then be used to select exploration targets.

Selected References

Adams, S. S., et al., 1974, Alteration of detrital magnetite-ilmenite in continental sandstones of the Morrison formation, New Mexico, in Formation of uranium ore deposits: Vienna, International Atomic Energy Agency, p. 219-253.

Bailey, R. V., 1969, Uranium deposits in the Great Divide Basin, Crooks Gap area, Fremont and Sweetwater counties, Wyoming: University of Wyoming Contributions to Geology, v. 8, no. 2, p. 105-120.

_____, 1972, Review of uranium deposits in the Great Divide Basin, Crooks Gap area, Wyoming: The Mountain Geologist, v. 9, no. 2-3, p. 165-182.

Collins, William, 1976, Spectroradiometric detection and mapping of areas enriched in ferric iron minerals using airborne and orbital measurements: New York, Columbia University Ph. D. thesis, 114 p.

Dahl, A. R., and Hagmaier, J. L., 1974, Genesis and characteristics of the Southern Powder River Basin uranium deposits, Wyoming, in Formation of uranium ore deposits: Vienna, International Atomic Energy Agency, p. 210-216.

Daniels, J. J., Scott, J. H., Blackmon, P. D., and Starkey, H. S., 1977, Borehole geophysical investigations in the South Texas uranium district: U.S. Geological Survey Journal Research, v. 5, no. 3, p. 343-357.

Deer, W. A., Howie, R. A., and Zussman, J., 1966, An introduction to the rock forming minerals: London, Longman Group Ltd., 528 p.

Denault, K. J., 1974, Origin of sandstone type uranium in Wyoming: Stanford, California, Stanford University Ph. D. thesis, 352 p.

Denson, N. M., and Pipringos, G. N., 1974, Geologic map and sections showing areal distribution of Tertiary rocks near the southeastern terminus of the Wind River Range, Fremont and Sweetwater Counties, Wyoming: U.S. Geological Survey Miscellaneous Geological Investigations Map I-835, scale of 1:48,000.

Files, F. G., 1970, Geology and alteration associated with Wyoming uranium deposits: Berkeley, California, University of California Ph. D. thesis, 113 p.

Folk, R. L., 1976, Reddening of desert sands: Simpson desert, N.T., Australia: Journal of Sedimentary Petrology, v. 46, no. 3, p. 604-615.

Gates, D. M., Keegan, H. J., Schleter, J. C., and Weidner, V. R., 1965, Spectral properties of plants: Applied Optics, v. 4, no. 1, p. 11-20.

Goetz, A. F. H., et al., 1975, Application of ERTS images and image processing to regional geologic problems and geologic mapping in Northern Arizona: Pasadena, Calif., California Institute Technology, Jet Propulsion Laboratory technical report 32-1597.

Granger, H. C., and Warren, C. G., 1974, Zoning in the altered tongue associated with roll-type uranium deposits, in Formation of uranium ore deposits: Vienna, International Atomic Energy Agency, p. 185-199.

Harshman, E. N., 1972, Uranium deposits of the Shirley Basin, Wyoming: The Mountain Geologist, v. 9, no. 2-3, p. 159-163.

_____1974, Distribution of elements in some roll-type uranium deposits, in Formation of uranium ore deposits: Vienna, International Atomic Energy Agency, p. 169-181.

Honey, F. R., Prelat, A., and Lyon, R. J. P., 1974, STANSORT: Stanford remote sensing laboratory pattern recognition and classification system, in Proceedings of Ninth International Symposium on Remote Sensing of Environment, Ann Arbor, Mich., p. 857-905.

Hunt, G. R., 1977, Spectral signatures of particulate minerals in the visible and near infrared: Geophysics, v. 42, no. 3, p. 501-513.

Hunt, G. R., and Ross, H. P., 1967, A bidirectional reflectance attachment for spectroscopic measurements: Applied Optics, v. 6, p. 1687-1690.

Hunt, G. R., and Salisbury, J. W., 1970, Visible and near-infrared spectra of minerals and rocks. I. Silicate minerals: Modern Geology, v. 1, p. 283-300.

_____1976, Visible and near-infrared spectra of minerals and rocks. WI. Sedimentary rocks: Modern Geology, v. 5, p. 211-217.

Hunt, G. R., Salisbury, J. W., and Lenhoff, C. J., 1971, Visible and near-infrared spectra of minerals and rocks. III. Oxides and hydroxides: Modern Geology, v. 2, p. 195-205.

_____1973, Visible and near-infrared spectra of minerals and rocks. VI. Additional silicates: Modern Geology, v. 4, p. 85-106.

Keefer, W. R., and Van Lieu, J. A., 1966, Paleozoic formations in the Wind River Basin, Wyoming: U.S. Geological Survey Professional Paper 495-B, 60 p.

Langden, R. E., and Kidwell, A. L., 1973, Geology and geochemistry of the Highland uranium deposit, Converse county, Wyoming: Wyoming Geological Association Earth Science Bulletin, December 1973, p. 41-48.

Love, J. D., 1970, Cenozoic geology of the Granite Mountains area, central Wyoming: U.S. Geological Survey Professional Paper 495-C, 154 p.

Lyon, R. J. P., 1977, Mineral exploration applications of digitally processed Landsat imagery, in Proceedings, First Annual W. T. Pecora Memorial Symposium, Oct. 28-31, 1975, Sioux Falls, S.D.: U.S. Geological Survey Professional Paper 1015, p. 271-292.

_____1976, Feasibility of using S-191 infrared spectra for geological studies from space: Stanford Univ. Remote Sensing Laboratory technical report 76-2.

Marrs, R. W., Breckenridge, R. M., Houston, R. S., and Root, F. K., 1973, Color anomalies, minerals, and ERTS-1 imagery: Univ. of Wyoming Contributions to Geology, v. 12, no. 2, p. 105-110.

Masursky, H., and Pipringos, G. N., 1959, Uranium-bearing coal in the Red Desert, Great Divide Basin, Sweetwater County, Wyoming: U.S. Geological Survey Bulletin 1055-G, p. 181-215.

Offield, T. W., 1976, Remote sensing in uranium exploration, in Exploration for uranium ore deposits: Vienna, International Atomic Energy Agency, p. 731-744.

Pipringos, G. N., 1968, Correlation and nomenclature of some Triassic and Jurassic rocks in south central Wyoming: U.S. Geological Survey Professional Paper 594-D, 26 p.

Reynolds, R. C., and Hower, J., 1970, The nature of interlayering in mixed-layer illite-montmorillonites: Clays and Clay Minerals, v. 18, p. 25-36.

Rowan, L. C., Wetlaufer, P. H., Goetz, A. F. H., Billingsley, F. C., and Stewart, J. H., 1974, Discrimination of rock types and altered areas in Nevada by use of ERTS images: U.S. Geological Survey Professional Paper 883, 35 p.

Rowan, L. C., Goetz, A. F. H., and Ashley, R. P., 1977, Discrimination of hydrothermally altered and unaltered rocks in visible and near infrared multispectral images: Geophysics, v. 42, no. 3, p. 522-535.

Rubin, B., 1970, Uranium roll front zonation in the southern Powder River Basin, Wyoming: Wyoming Geological Association Earth Science Bulletin, December 1970, p. 5-12.

Salmon, B., and Vincent, R. K., 1974, Surface compositional mapping in the Wind River Range and Basin, Wyoming, by multispectral techniques applied to ERTS-1 data, in Proceedings of Ninth International Symposium on Remote Sensing of Environment, Ann Arbor, Mich., p. 2005.

Salmon, B., and Pillars, W., 1975, Multispectral processing of Landsat data for uranium exploration in the Wind River Basin, Wyoming: A visible region ratio to enhance surface alteration associated with roll-type uranium deposits: U.S. Energy Research and Development Administration Open-File Report GJO-1635-1.

Schmitt, L. J., Jr., 1976, Geologic map of the Sagebrush Park quadrangle, Wyoming: U.S. Geological Survey Open-File Report 76-676, 1:24,000 scale.

_____1977, Preliminary geologic map of the Crooks Peak quadrangle, Wyoming: U.S. Geological Survey Open-File Report 77-322, 1:24,000 scale.

Spirakis, C. S., and Condit, C. D., 1975,Preliminary report on the use of Landsat-1 reflectance data in locating alteration zones associated with uranium mineralization near Cameron, Arizona: U.S. Geological Survey Open-File Report 75-416.

Stephens, J. G., 1964, Geology and uranium deposits at Crooks Gap, Fremont County, Wyoming: U.S. Geological Survey Bulletin 1147-F, 82 p.

Valley, S. L., eds., 1965, Handbook of geophysics and space environments; U.S. Air Force Cambridge Research Laboratories, Bedford, Mass.: New York, McGraw-Hill Book Col, p. 16-2 to 16-9.

Walker, T. R., 1976, Diagenetic origin of continental red beds, in Falke, H., ed., The continental Permian in central, west and southern Europe: Dordrecht-Holland, D. Reidel Publishing Co., p. 240-282.

Appendix 1

Laboratory Data

Mineralogical Data

[Sample descriptions are given in the following pages. The presence of a mineral is denoted by an x, the absence by a blank; a query denotes identification uncertain; "undet" means undetermined, i.e., no data; "tr" is for trace, or very low quantities.]

Sample	Quartz	Alkali feldspar	Kaolinite	Illite	Montmorillonite	Mixed-layer illite, montmorillonite	% montmorillonite in mixed-layer clays	Undifferentiated iron oxides	Iron-rich chlorites	Hematite	Total iron as % Fe_2O_3	FeO %
CG76-35	x	x	x	x	x	x	60	x		?	0.60	0.06
CG77-1(R)	x	x	x		x	x	50-60	x		?	0.68	0.05
CG77-5	x	x	x		x	x	50-60	x		?	1.71	0.47
CG76-21	x	x	x	x				x		?	1.35	0.41
CG76-32	x	x	x	x	x	x	undet	x		?	5.49	0.69
CG77-1(B)	x	x	x	x	x	x	80				0.36	0.05
CG77-11(B)	x	x	x		x	x	80				0.81	0.13
CG76-86	x	x	x						x	x	6.36	1.56
CG76-60	x	x	x		x	x	80	tr			0.99	0.41
CG76-52b	x	x	x	x							1.25	1.03
CG77-9b	x	x	x		x	x	80				0.75	0.26
CG77-13c	x	x	x		x	x	80				1.75	0.07
CG77-15b	x	x	x		x	x	60-80				0.05	0.16
CG76-1	x	x						tr		?	0.28	0.07

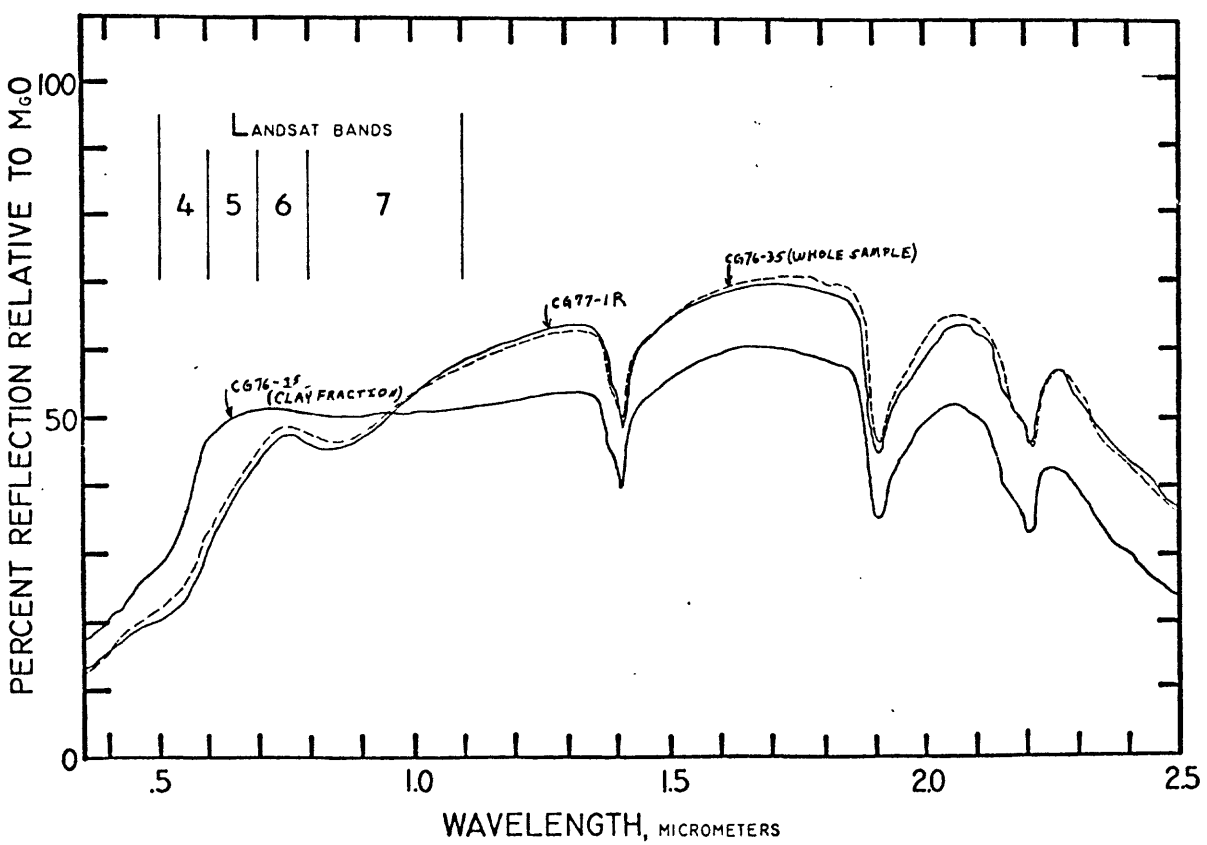

Figure 11.--Fresh red-colored alteration. Sample CG76-35: Pale to moderate red arkosic soil developed on altered Battle Spring Formation. This is a sample of the typical altered material used as a prospecting guide. Sample CG77-1(R): Pale to moderate red arkosic soil developed on altered Battle Spring Formation. Sample from same locality as CG76-35.

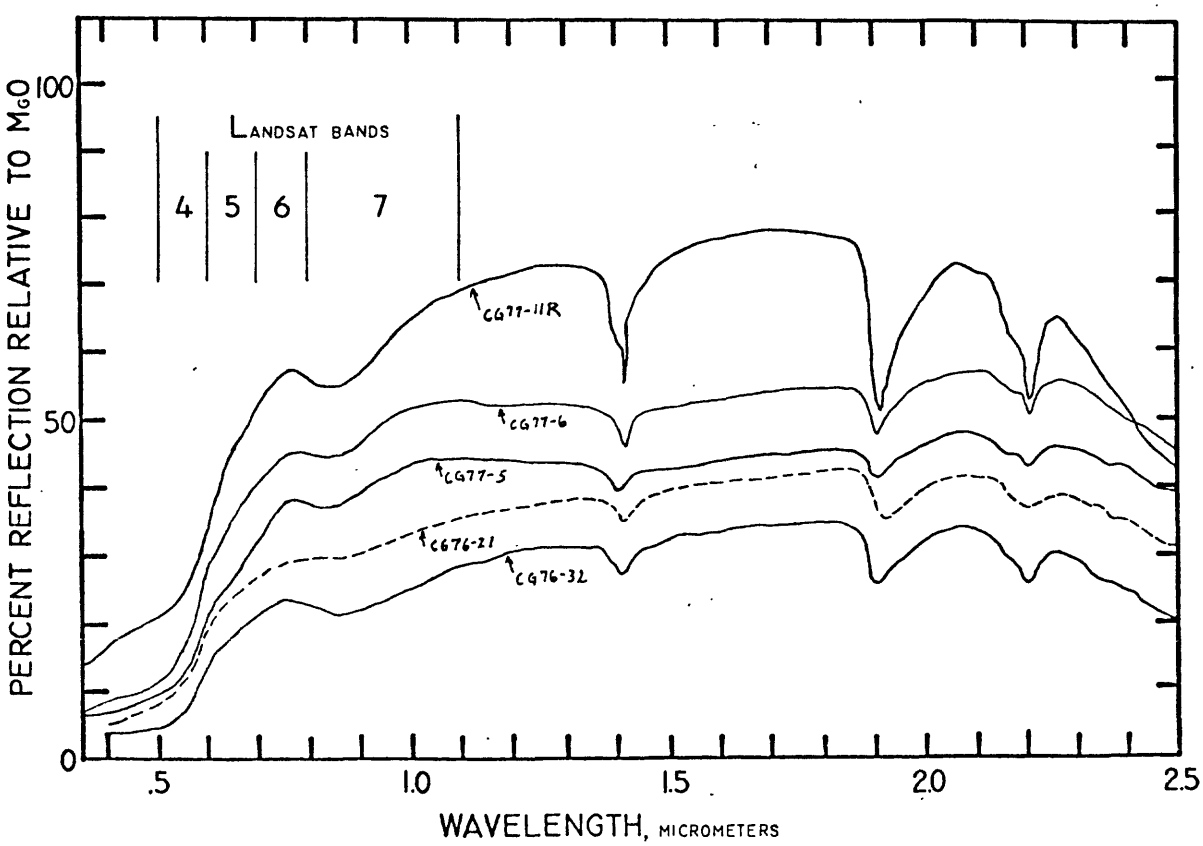

Figure 12.--Red alteration. Sample CG77-5: Moderate-reddish-brown sandy soil developed on altered Battle Spring Formation. Naturally weathered exposure. Sample CG77-6: Moderate-red sandy soil developed on altered Battle Spring Formation. Naturally weathered exposure. Sample CG77-11(R): Pale- to moderate-red arkosic soil developed on altered Battle Spring Formation. See CG77-11(B) for comparison with bleached alteration at the same locality. Sample CG76-21: Light-brown sandy soil with quartz and feldspar lithics. Fresh alteration not exposed here at the surface. Sample CG76-32: Moderate-reddish-brown sandy soil. Weathered red-colored alteration of the Battle Spring Formation.

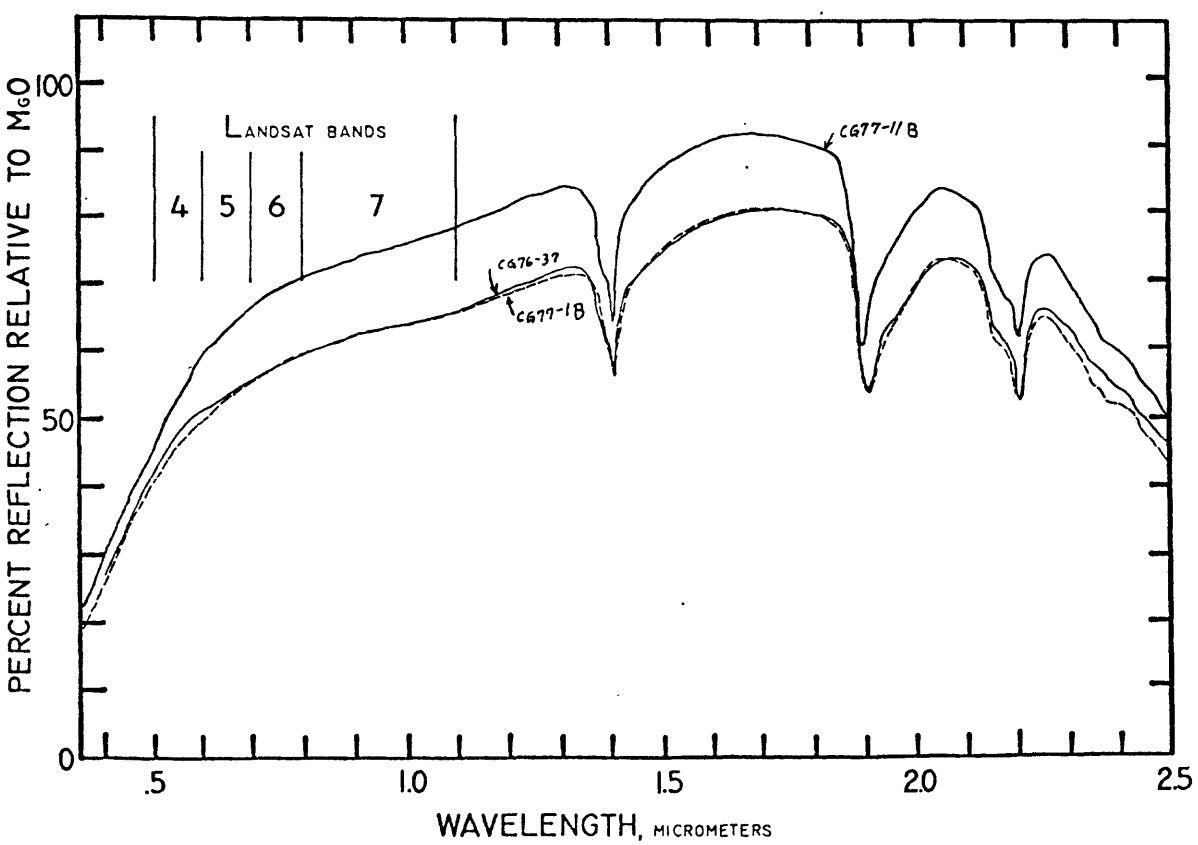

Figure 13.--Bleached alteration. Sample CG76-37: Very pale orange arkosic soil developed on bleached alteration of Battle Spring Formation. No iron staining. Same locality as CG76-35. Sample CG77-1(B): Light-yellowish-gray arkosic soil developed on bleached alteration of Battle Spring Formation. Sample CG77-11(B): Light-yellowish-gray arkosic soil developed on bleached alteration of Battle Spring Formation.

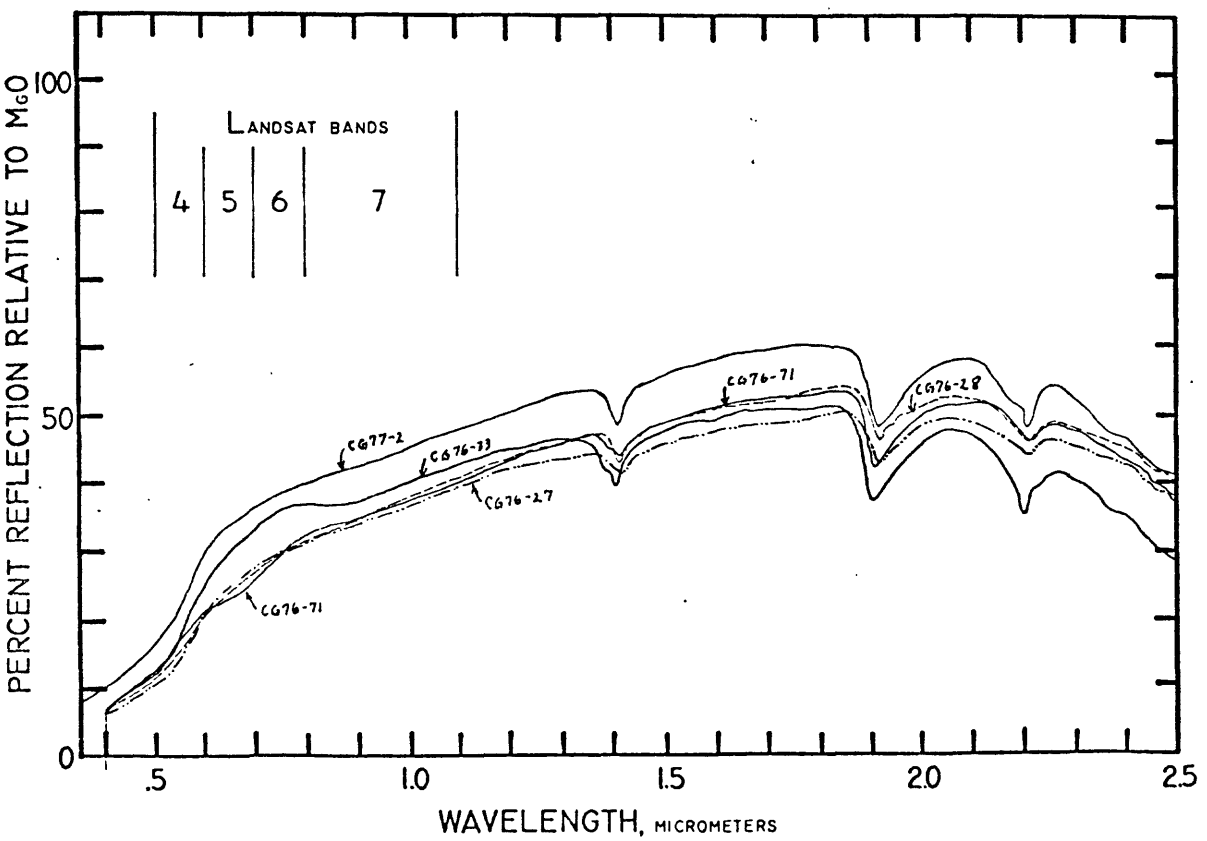

Figure 14.--Weathered red alteration. Sample CG76-27: Moderate-yellowish-brown sandy soil with fine to coarse sand grains. Soil developed on altered Battle Spring Formation. Sample CG76-28: Moderate-yellowish-brown sandy soil with coarse, angular lithics. Soil developed on altered Battle Spring Formation. Sample CG76-33: Light-brown sandy soil. Soil developed on altered Battle Spring Formation. Sample CG 76-71: Yellowish-gray sandy soil. Very fine to medium grain size with some dead vegetation and pebbles. Soil developed on altered Battle Spring Formation. Sample CG77-2: Grayish-orange sandy soil. Quartz and feldspar lithics with quartzite cobbles and granitic boulders. Developed on altered Battle Spring Formation.

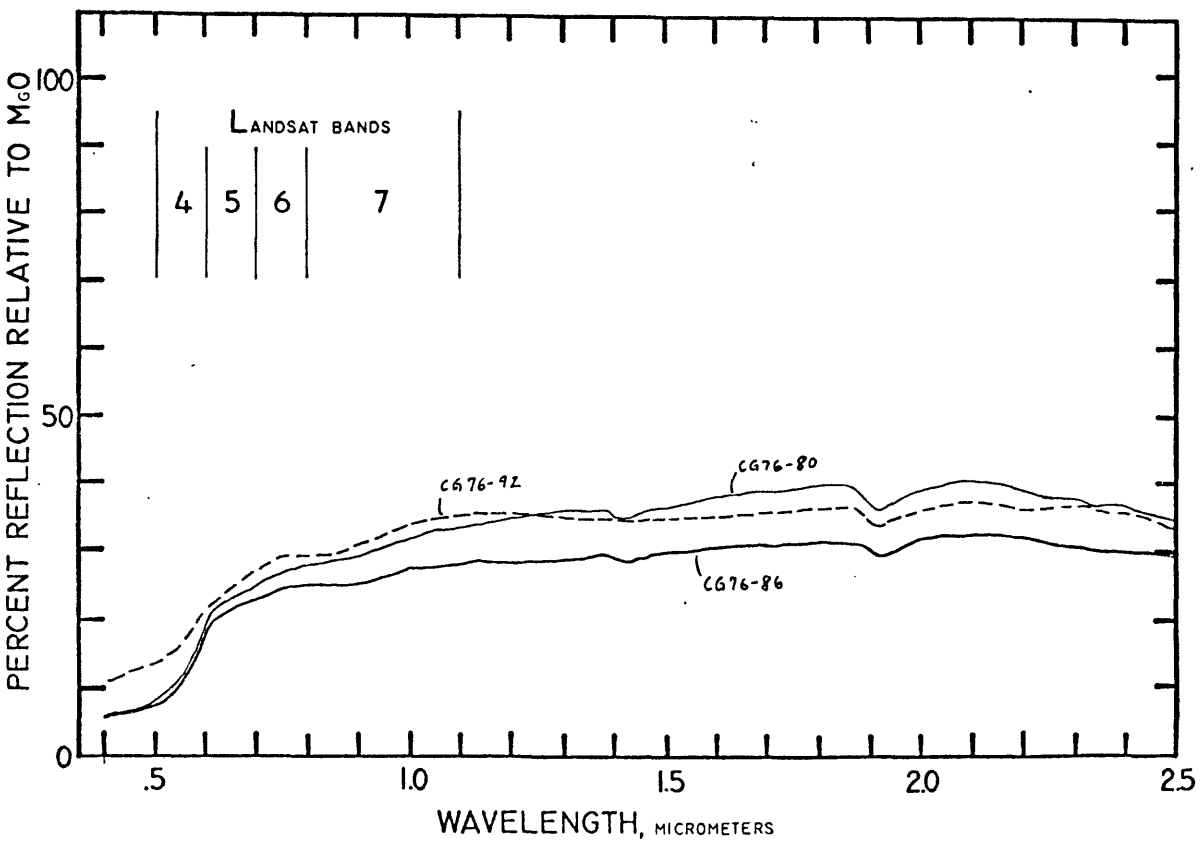

Figure 15.--Red Paleozoic rocks. Sample CG76-80: Light-brown soil with limestone pebbles. Chugwater Group outcrops. Sample CG76-86: Moderate-reddish-brown soil with shale fragments. Chugwater Group outcrops. Sample CG76-92: Undivided Cambrian sediments. A medium to very coarse grained quartzite. Sorting of grains in Cambrian quartzite is poor. Color is a pale red. The spectra presented here is of the weathered surface.

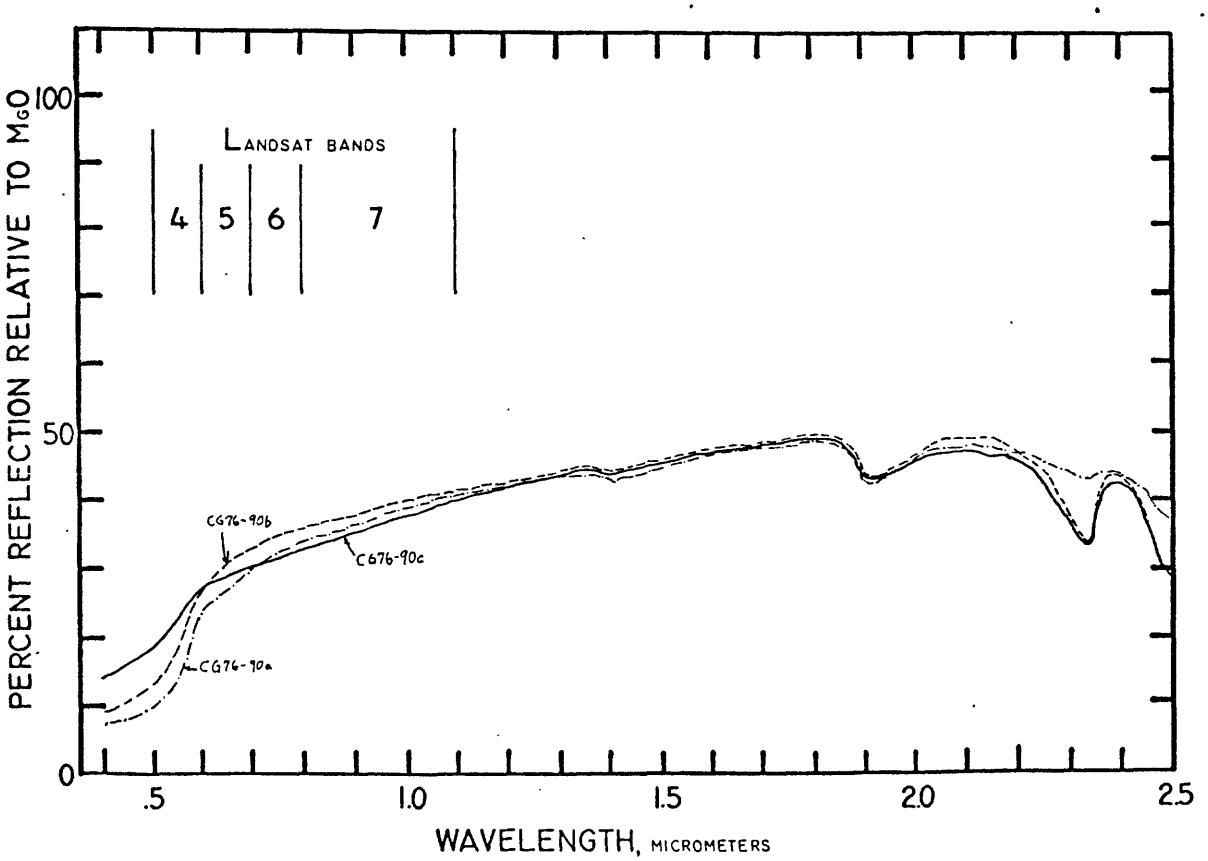

Figure 16.--Red-stained limestone. Sample CG76-90: Limestone of Chugwater Group. Weathered surface naturally etched and stained light brown. (a) Light-brown stained, weathered surface; (b) weathered wurface with less staining; (c) weathered surface with no staining.

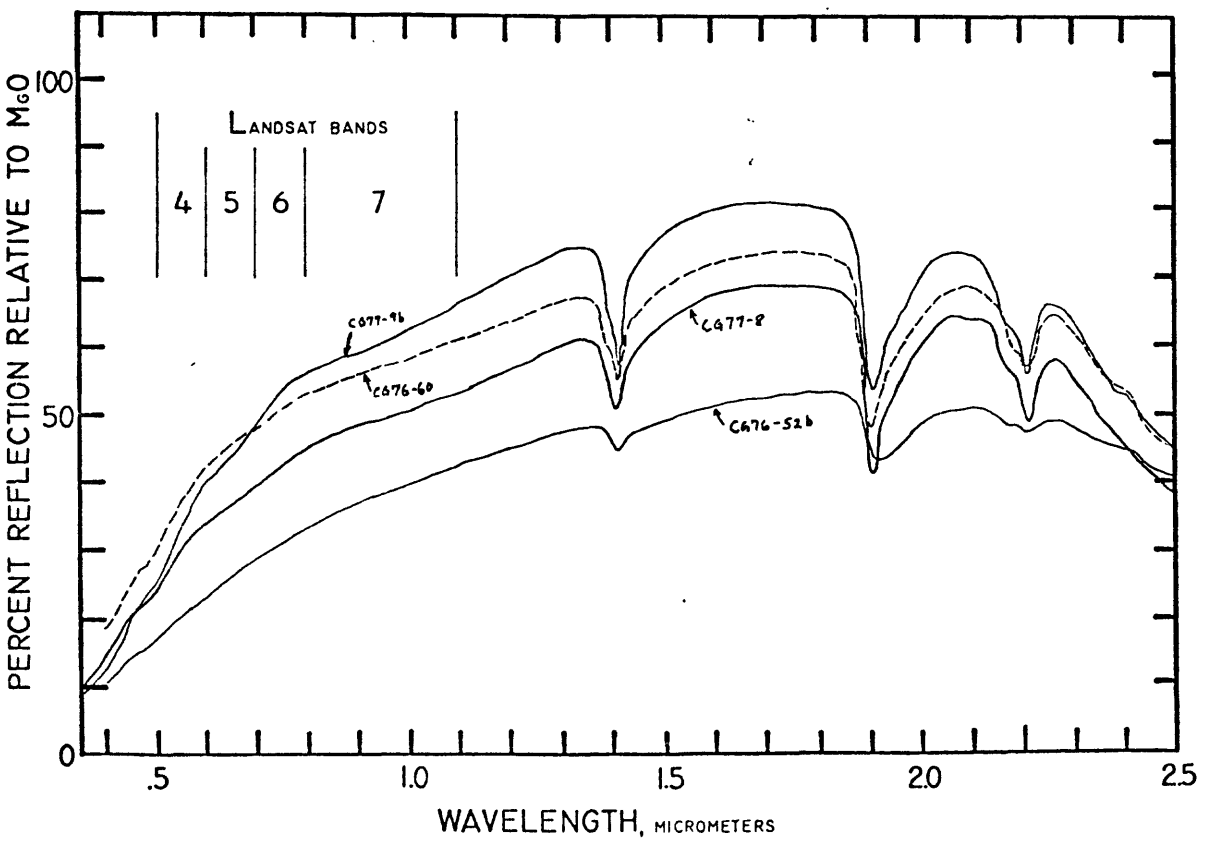

Figure 17.--Unaltered Battle Spring Formation. Sample CG77-8: Yellowish-gray soil with granite fragments and cobbles. Developed on unaltered Battle Spring Formation. Sample CG77-9b: Grayish-orange soil with granite fragments and cobbles. Developed on unaltered Battle Spring Formation. This sample shows typical yellowish soil color of unaltered areas. Sample CG76-52b: Grayish-orange powdery soil with coarse-grained granitic fragments. Developed on unaltered Battle Spring Formation. Sample CG76-60: Grayish-orange soil with coarse-grained granitic fragments. Developed on unaltered Battle Spring Formation. Slight absorption is probably due to iron staining related to weathering of iron in mafic minerals.

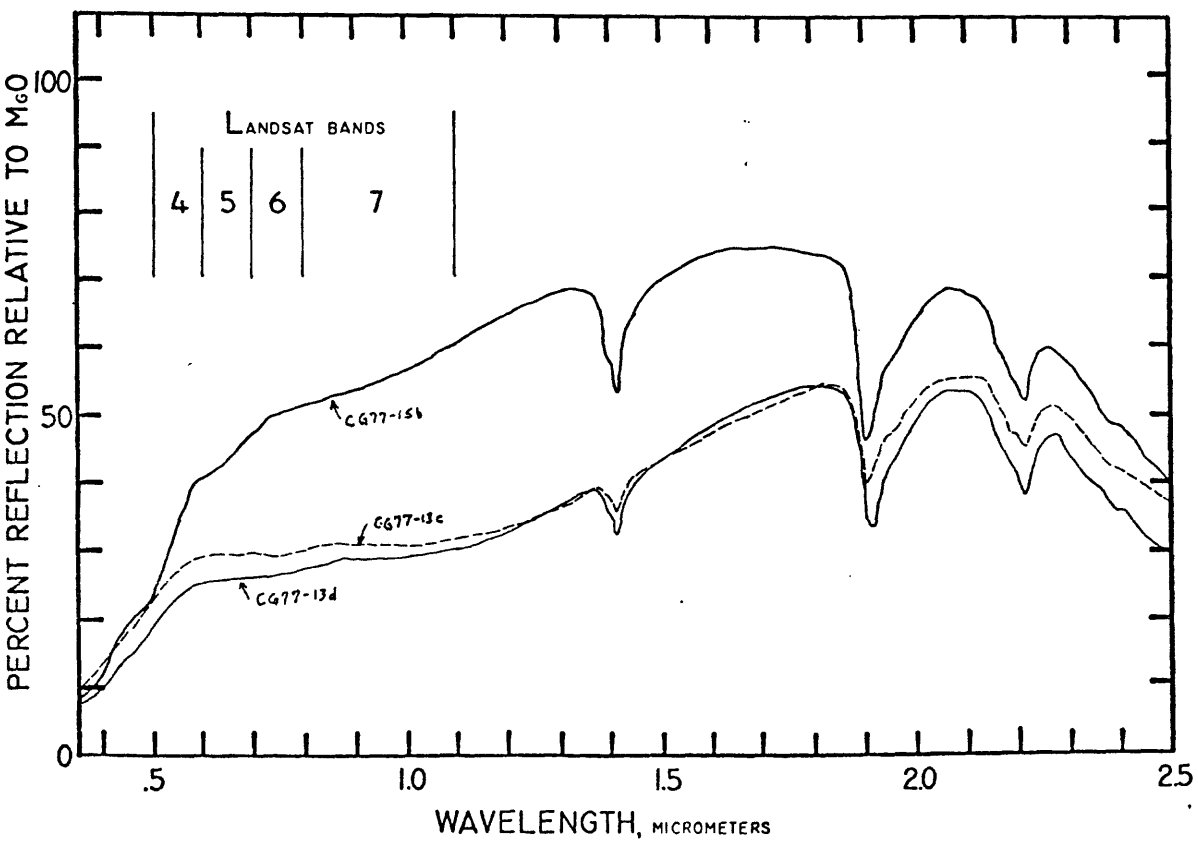

Figure 18.--Unaltered Battle Spring Formation. Sample CG77-13c: Pale-olive-colored, clay-rich, unconsolidated, fine-grained arkose washed from a bulldozer cut in the unaltered Battle Spring Formation. Typical of "reduced" host rock found in hillside cuts and trenches. Sample: CG77-13d: Grayish-yellow soil with granitic fragments and some dead vegetation. This soil developed on unaltered Battle Spring Formation on hillslope above locality of CG77-13c. Sample CG77-15b: Grayish-orange, coarse, poorly cemented arkosic material of unaltered Battle Spring Formation.

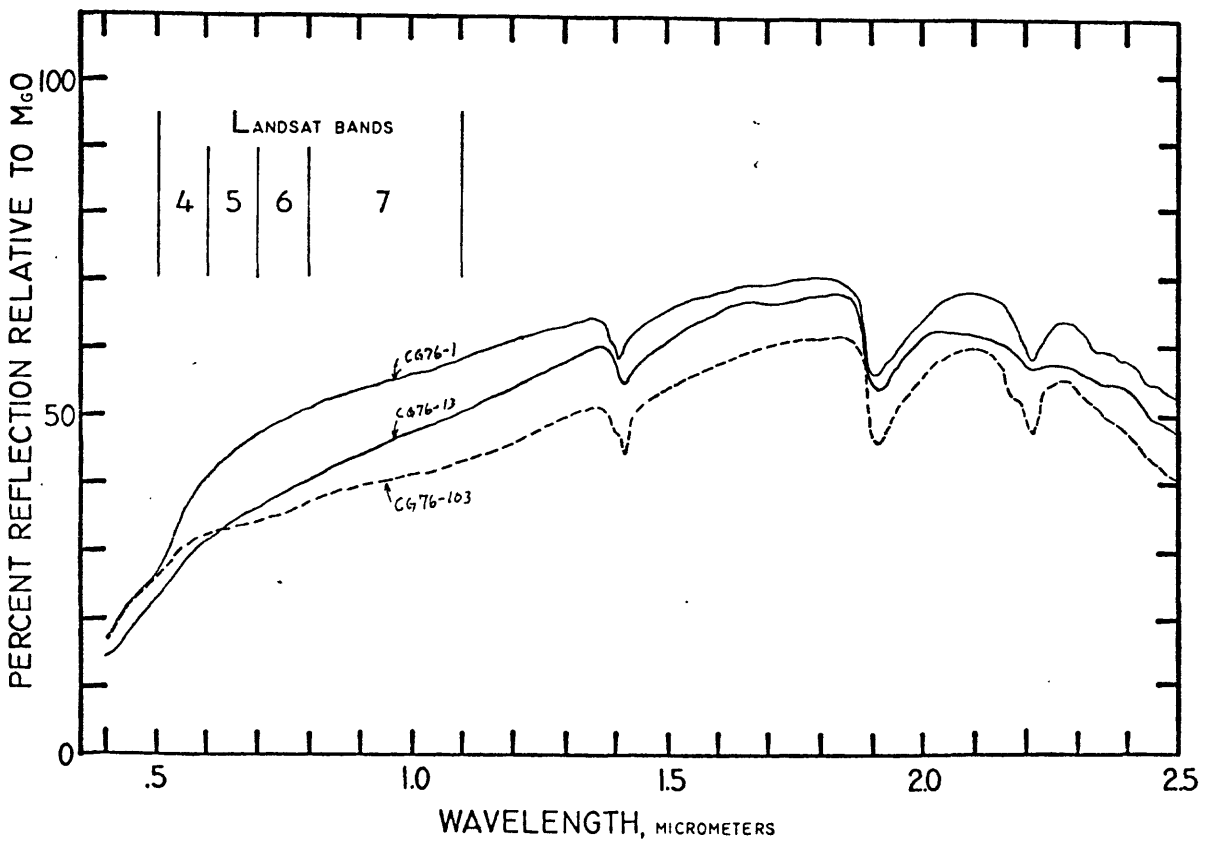

Figure 19.--Sand dunes and mine dumps. Sample CG76-1: Very pale yellow quartz sand from sand dunes. Quartz grains are rounded, frosted, and slightly stained with iron oxides. Sample CG76-13: Similar to CG76-1 but also contains some dead vegetation. Sample CG76-103: Surface sample of material from dump of Seismic open-pit mine. Contains fine to coarse sand and pebbles and is a yellowish gray in color.

Appendix 2

Simulated Landsat Data

[The following are the values simulated from the laboratory samples for Landsat bands 4, 5, 6, 7, and band ratios 5/4, 6/5, 7/5, and 7/6. The band values are in units of watts per square centimeter. The samples have been described in Appendix 1.]

Sample	4	5	6	7	5/4	6/5	7/5	7/6
			Fresh red alteration					
77-1R	27.36	34.98	37.12	50.99	1.28	1.06	1.46	1.37
76-35	29.78	36.30	38.37	51.76	1.22	1.06	1.46	1.35
77-11R	29.55	41.76	44.70	61.71	1.41	1.07	1.48	1.38
			Weathered red alteration					
77-6	21.03	32.68	35.11	49.61	1.55	1.07	1.52	1.41
77-5	15.59	25.05	29.31	41.46	1.61	1.17	1.66	1.41
76-21	13.88	21.67	22.96	32.38	1.56	1.06	1.49	1.41
76-32	9.31	16.84	18.23	24.14	1.81	1.08	1.43	1.32
77-2	25.92	30.65	31.14	45.42	1.18	1.02	1.48	1.46
76-33	20.67	27.32	28.77	40.06	1.32	1.05	1.47	1.39
76-27	16.88	22.82	24.05	36.01	1.35	1.05	1.58	1.50
76-71	18.95	21.10	23.85	36.94	1.11	1.13	1.75	1.55
76-28	17.52	22.01	23.83	36.74	1.26	1.08	1.67	1.54
			Bleached alteration					
76-37	53.67	48.06	46.58	65.69	0.90	0.97	1.37	1.41
77-1B	51.67	47.56	46.52	65.68	0.92	0.98	1.38	1.41
77-11B	60.58	57.36	55.97	78.13	0.95	0.98	1.36	1.40
			Unaltered red rocks					
76-92	18.62	22.19	23.04	32.74	1.19	1.04	1.48	1.42
76-80	13.90	20.68	21.47	31.22	1.49	1.04	1.51	1.45
76-86	12.43	19.13	19.44	27.10	1.54	1.02	1.42	1.39
76-90B	22.28	27.85	28.21	40.42	1.25	1.01	1.45	1.43
76-90A	17.28	25.28	26.04	38.58	1.46	1.03	1.53	1.48
			Unaltered non-red rocks					
77-9B	38.02	40.34	43.09	62.94	1.06	1.07	1.56	1.46
76-60	41.81	41.12	41.16	59.45	0.98	1.00	1.45	1.44
77-8	33.60	33.21	34.26	50.95	0.99	1.03	1.53	1.49
76-52B	22.70	23.76	25.11	39.05	1.05	1.06	1.64	1.56
77-15B	38.59	39.75	40.34	57.21	1.03	1.01	1.44	1.42
77-13C	30.25	26.11	23.84	32.57	0.86	0.91	1.25	1.37
77-13D	25.57	22.78	21.36	30.12	0.89	0.94	1.32	1.41
76-1	39.54	40.08	39.74	57.13	1.01	0.99	1.43	1.44
76-13	31.04	30.78	31.10	46.80	0.99	1.01	1.52	1.50
76-103	33.70	29.86	28.66	41.78	0.89	0.96	1.40	1.46

The following are the solar irradiance and Landsat band response values that are multiplied by the laboratory reflectance values (in percent per wavelength interval) and summed over each filter width to obtain the four MSS band values for each sample (which are listed above). Wavelength is in units of micrometers, solar spectral irradiance in watts per square centimeter per micrometer, and total band response is a fraction of unity, that is 0.99 means 99 percent.

Landsat band response values are from Hovis (in a written communication to R. J. P. Lyon). The solar irradiance values are from the Air Force Cambridge Research Laboratory Geophysics Handbook (Valley, 1965) table 16-4 (solar irradiance at sea level with an air mass of 2).

Wavelength	Solar irrad.	Band response
Landsat MSS four:		
(filter width: 0.48 to 0.65 μm)		
0.48	1183	0.0
0.49	1210	0.150
0.50	1215	0.590
0.51	1206	0.830
0.52	1199	0.927
0.53	1188	0.970
0.54	1198	0.995
0.55	1190	0.990
0.56	1182	0.994
0.57	1178	0.986
0.58	1168	0.968
0.59	1161	0.726
0.60	1167	0.269
0.61	1168	0.080
0.62	1165	0.012
0.63	1176	0.002
0.64	1175	0.0
0.65	1173	0.0

Wavelength	Solar irrad.	Band Response
Landsat MSS five:		
(filter width: 0.58 to 0.76 μm)		
0.58	1168	0.0
0.59	1161	0.0
0.60	1167	0.091
0.61	1168	0.456
0.62	1165	0.772
0.63	1176	0.844
0.64	1175	0.867
0.65	1173	0.854
0.66	1166	0.791
0.67	1160	0.730
0.68	1149	0.731
0.69	978	0.748
0.70	1108	0.545
0.71	1070	0.210
0.72	832	0.097
0.73	965	0.046
0.74	1041	0.020
0.75	867	0.005
0.76	566	0.0

Wavelength	Solar irrad.	Band response
Landsat MSS six:		
(filter width: 0.67 to 0.85 μm)		
0.67	1160	0.0
0.68	1149	0.059
0.69	978	0.250
0.70	1108	0.587
0.71	1070	0.819
0.72	832	0.893
0.73	965	0.896
0.74	1041	0.858
0.75	867	0.802
0.76	566	0.780
0.77	968	0.787
0.78	907	0.791
0.79	923	0.645
0.80	857	0.357
0.81	698	0.171
0.82	801	0.074
0.83	863	0.029
0.84	858	0.003
0.85	839	0.0

Wavelength	Solar irrad.	Band response
Landsat MSS seven:		
(filter width: 0.77 to 1.09 μm)		
0.7	968	0.0
0.78	907	0.02
0.79	923	0.029
0.80	857	0.298
0.81	698	0.909
0.82	801	0.943
0.83	863	0.964
0.84	858	0.984
0.85	839	0.977
0.86	813	0.966
0.87	798	0.933
0.88	614	0.899
0.89	517	0.857
0.90	480	0.825
0.91	375	0.785
0.92	258	0.730
0.93	169	0.680
0.94	278	0.631
0.95	487	0.581
0.96	584	0.533
0.97	633	0.496
0.98	645	0.456
0.99	643	0.421
1.00	630	0.384
1.01	620	0.339
1.02	610	0.302
1.03	601	0.266
1.04	592	0.226
1.05	551	0.191
1.06	526	0.150
1.07	519	0.119
1.08	512	0.089
1.09	514	0.055

Appendix 3

Landsat data

[Data used are uncorrected Landsat radiance values (raw DN values). Site letter designations refer to locations given on the CRC. The Landsat scene ID is #-1013-17300, imaged on August 5, 1972, with the sun at an elevation of 55 degrees and an azimuth of 128 degrees.]

Site U Unaltered Battle Spring Formation No. samples = 112

	Mean	Standard deviation	Percent standard deviation/mean
Band 4	39.35	2.445	6.213
Band 5	43.77	2.878	6.574
Band 6	45.95	2.631	5.726
Band 7	42.91	2.006	4.677
Ratio 7/6	0.935	.036	3.870
Ratio 7/5	0.982	.044	4.492
Ratio 7/4	1.092	.058	5.285
Ratio 6/5	1.051	.044	4.172
Ratio 6/4	1.169	.050	4.290
Ratio 5/4	1.112	.040	3.598

Unconsolidated, weathered, unaltered Battle Spring Formation arkose with a covering of low sagebrush and grasses. Moderate vegetation density. Granitic pebbles of the arkose are frequently stained with iron oxides from the weathering of mafic minerals.

Site C Triassic Chugwater Group red beds No. Samples = 18

	Mean	Standard deviation	Percent standard deviation/mean
Band 4	38.22	1.699	4.446
Band 5	48.55	2.791	5.748
Band 6	51.61	3.583	6.942
Band 7	45.11	2.494	5.529
Ratio 7/6	0.875	.039	4.448
Ratio 7/5	0.931	.058	6.285
Ratio 7/4	1.182	.078	6.588
Ratio 6/5	1.064	.067	6.309
Ratio 6/4	1.352	.106	7.857
Ratio 5/4	1.270	.056	4.408

Chugwater Group shales and limestones exposed along a low ridge, with weathering products washing to either side of the ridge. Vegetation is sparse, consisting mostly of low sagebrush and grasses.

Site A Exposed alteration No. samples = 6

	Mean	Standard deviation	Percent standard deviation/mean
Band 4	61.16	5.913	9.667
Band 5	80.66	8.936	11.07
Band 6	83.66	6.592	7.879
Band 7	71.33	5.887	8.253
Ratio 7/6	0.852	.019	2.280
Ratio 7/5	0.887	.032	3.633
Ratio 7/4	1.168	.050	4.313
Ratio 6/5	1.040	.038	2.630
Ratio 6/4	1.370	.042	3.055
Ratio 5/4	1.317	.049	2.693

The floor of the Snobal open pit mine (inactive). Exposed, altered Battle Spring Formation rocks; the pale-red color of the alteration is ubiquitous. There is no vegetation.

Site T Seismic dump No. samples = 18

	Mean	Standard deviation	Percent standard deviation/mean
Band 4	78.22	4.570	5.842
Band 5	87.55	6.298	7.193
Band 6	81.61	3.942	4.831
Band 7	69.00	3.307	4.793
Ratio 7/6	0.846	.023	2.719
Ratio 7/5	0.789	.028	3.569
Ratio 7/4	0.883	.034	3.860
Ratio 6/5	0.934	.035	3.719
Ratio 6/4	1.044	.036	3.491
Ratio 5/4	1.118	.029	2.623

The leveled top of the dump of the Seismic open pit mine. (This area of the mine dump is not used.) There is no vegetation. The color is dominantly a pale yellowish gray.

Site G Green Mountain pine forest No. samples = 104

	Mean	Standard deviation	Percent standard deviation/mean
Band 4	20.60	1.668	8.098
Band 5	16.56	2.330	14.06
Band 6	28.62	2.264	7.912
Band 7	30.88	2.626	8.504
Ratio 7/6	1.080	.061	5.654
Ratio 7/5	1.884	.202	10.70
Ratio 7/4	1.502	.113	7.534
Ratio 6/5	1.748	.193	11.05
Ratio 6/4	1.393	.112	8.068
Ratio 5/4	0.803	.072	9.014

This site is a dense stand of lodgepole pine on Green Mountain.

Site S Sagebrush No. samples = 36

	Mean	Standard deviation	Percent standard deviation/mean
Band 4	36.11	2.108	5.838
Band 5	39.69	2.149	5.413
Band 6	44.97	2.273	5.056
Band 7	44.00	1.971	4.480
Ratio 7/6	0.979	.032	3.310
Ratio 7/5	1.110	.053	4.813
Ratio 7/4	1.221	.073	6.003
Ratio 6/5	1.134	.048	4.228
Ratio 6/4	1.247	.062	4.940
Ratio 5/4	1.100	.034	3.075

High, dense sagebrush on Crooks Gap Conglomerate on Green Mountain.

Site M Hill north of mine area No. samples = 24

	Mean	Standard deviation	Percent standard deviation/mean
Band 4	46.37	3.751	8.088
Band 5	58.12	4.830	8.310
Band 6	63.29	5.819	9.194
Band 7	57.16	4.526	7.918
Ratio 7/6	0.904	.029	3.267
Ratio 7/5	0.985	.048	4.929
Ratio 7/4	1.235	.081	6.600
Ratio 6/5	1.089	.055	5.013
Ratio 6/4	1.366	.099	7.229
Ratio 5/4	1.253	.041	3.242

A large hill underlain by altered Battle Spring Formation, to the north of Sheep Mountain. Extensive exploration has left numerous roads and bulldozer cuts exposing pale-red-colored, altered Battle Spring rocks. The surface consists of the weathered rock unit with the finer material removed, leaving a pebbly "pavement" surface. The pebbles at the surface and the finer material below are dark brownish red in color. The surface is covered sparsely with low sagebrush and grasses.

Site D Sand dunes SE of Crooks Gap No. samples = 16

	Mean	Standard deviation	Percent standard deviation/mean
Band 4	79.25	5.322	6.716
Band 5	96.87	6.561	6.772
Band 6	99.75	4.123	4.133
Band 7	90.00	3.932	4.369
Ratio 7/6	0.903	.031	3.384
Ratio 7/5	0.932	.066	7.142
Ratio 7/4	1.139	.077	6.736
Ratio 6/5	1.032	.051	4.969
Ratio 6/4	1.261	.055	4.360
Ratio 5/4	1.222	.032	2.595

Areally extensive sand dunes generally barren of vegetation, except around margins.
